

PART B: ANALYTICAL MODELING

by

J. R. Bellan
P. T. Harsha
R. B. Edelman

Science Applications, Inc. (SAI)
Combustion Dynamics and Propulsion Technology Division
20335 Ventura Boulevard, Suite 423
Woodland Hills, California 91364

TABLE OF CONTENTS

<u>Section</u>	<u>Page</u>
SUMMARY	80
I. COMPUTATIONAL METHODS FOR RECIRCULATING REACTING FLOWS.	83
A. Stream Function - Vorticity Methods	83
B. Pressure Velocity Methods	88
C. Finite-Element Methods.	92
D. Approximate Methods (Modular Models).	93
E. Summary of Required Work: Analytical Models.	95
II. TURBULENT FLOW MODELING AND THE PHENOMENON OF UNMIXEDNESS.	96
A. Turbulent Kinetic Energy Model.	96
B. Unmixedness	97
C. Summary of Required Work: Unmixedness Models	110
III. DROPLET AND SPRAY COMBUSTION.	111
A. Droplet Modeling.	111
B. Spray Combustion.	115
REFERENCES FOR SECTIONS I, II, III	117
IV. FUEL DECOMPOSITION AND COMBUSTION	123
A. Fuel Decomposition	123
B. Fuel Oxidation	130
REFERENCES FOR SECTION IV	135

SUMMARY

This report represents the results of a survey of the state-of-the art of combustion modeling. Particular attention is devoted to delineating the requirements for additional work needed to develop *practical* models of the combustion process of coal and shale liquids.

The report covers two main areas including:

1. Combustor modeling covering
 - a. treatment of the full elliptic equations
 - b. modular modeling
 - c. turbulence modeling
 - d. droplet and spray modeling
2. Fuel decomposition and combustion kinetics covering
 - a. pure pyrolysis
 - b. oxidative pyrolysis
 - c. soot formation
 - d. soot oxidation
 - e. vapor phase oxidation

The survey shows that the existing knowledge and utility of the various aspects of combustion modeling can be ranked as follows:

Combustion Modeling

1. Equation framework
 - a. modular
 - b. solutions of the unified elliptic equations
2. Turbulence
 - a. TKE methods-gas phase
 - b. gas phase unmixedness models
 - c. multiphase turbulence modeling
3. Multiphase combustion
 - a. single droplet
 - b. spray combustion

Fuel Decomposition and Combustion

1. Gas phase kinetics
 - a. high H/C
 - b. low H/C

2. Soot oxidation
 - a. global
3. Pyrolysis
 - a. global decomposition rates
 - b. products of decomposition
 - c. detailed kinetics
4. Soot formation
 - a. global
 - b. detailed

The results of the survey and ranking suggest that modular modeling should be emphasized while unified solutions of the full elliptic equations require longer term developments. In particular the work should proceed as follows:

1. Exploitation of the modular approach, with emphasis on the modeling of the shear layer region which couples the parabolic (directed flow) and stirred reactor (recirculation zone) modules.
2. Continued development of elliptic formulation with emphasis on the treatment of boundary conditions and the use of locally nonuniform grids. The application of the modular approach, i.e., models for specific flow regions (jets, recirculation zones) within an overall elliptic problem formulation should be pursued.

The survey results also show that the use of turbulent kinetic energy (TKE) models to obtain the mean flowfield in *gas phase* reacting flow situations is well established. However, the description of the effects of turbulent fluctuations on the local micro-scale (i.e., "molecular") mixing requires further development. This work should proceed as follows:

1. For flowfields which are spatially homogeneous in the mean, for example, stirred reactors, the use of two-environment and Monte Carlo methods to describe the microscale gas phase unmixedness should be pursued.
2. For spatially nonhomogeneous flows (jets, diffusion flames, general combustion chamber flows) the limits of applicability of probability distribution function techniques should be carefully assessed. In flows for which PDF techniques are not applicable, the development of direct solutions of the correlation equations should be continued.

Furthermore, turbulence modeling for *two phase* flows and spray modeling is required and should proceed as follows:

1. Application of one- and two-equation TKE models to diffusion flames.
2. Residence time averaging for sprays in recirculation zones.
3. Droplet and spray modeling with emphasis on surface kinetics including pyrolysis, partial oxidation, finite rate vaporization, and radiation.

In addition, the survey suggests that practical modeling of the chemical kinetics of decomposition and oxidation can be developed through quasiglobal modeling while full detailed kinetics and mechanism definition require longer term developments. The areas requiring particular attention are:

1. Pyrolysis and oxidative pyrolysis of hydrocarbon mixtures - measurements of Arrhenius parameters are needed.
2. Soot formation - quantity and size distribution of soot particles and Arrhenius parameters for soot formation (global reaction) need to be determined from measurements.
3. Fuel oxidation in conjunction with fuel pyrolysis - Arrhenius parameters for the global reaction rates are needed over a spectrum of equivalence ratios, temperatures ($800^{\circ} < T < 1500$ K) and pressures ($1 \leq P \leq 15$ atm).

In general, work reported here shows that practical near term models are needed and can be developed that will be applicable to all fuels in general and to coal and shale liquids (and gases) in particular.

ANALYTICAL MODELING OF CONTINUOUS FLOW COMBUSTORS

A general calculation procedure for a combustor flowfield must involve models for a number of complex physical and chemical processes, including turbulent recirculating flow, possibly with swirl, finite-rate chemical kinetics, droplet evaporation and combustion, and others. The development of such a procedure is clearly a formidable problem; however, considerable progress has been made in recent years in the development of calculation methods. In this section the application of a number of recently reported methods to the calculation of combustor flowfields is discussed. Because the primary difficulty involved in such computation is the numerical problem of computing turbulent recirculating flows, the emphasis in this discussion is on the numerical procedures that have been developed; however, the question of turbulence modeling and the related phenomenon of unmixedness will also be considered.

I. COMPUTATIONAL METHODS FOR RECIRCULATING REACTING FLOWS

Since most practical combustor flowfields involve large regions of recirculating flow, in which axial diffusion is important, direct calculation of these flows involves the numerical solution of the elliptic form of the governing equations. A considerable amount of research effort has been put into the development of numerical techniques for the solution of the elliptic equations of motion in recent years; some of this work and its application to combustor flow problems is described in the following.

A. Stream Function-Vorticity Methods

A widely used numerical technique for the solution of the elliptic equations of motion is the stream function-vorticity method based on the work of Gosman, et. al., (1) and known in some of its later versions by the acronym PISTEP. Instead of solving for the velocity components and the pressure field directly, in this method the pressure is eliminated as a variable through differentiation of the velocity component equations, resulting in linked equations for the stream function and vorticity. However, this procedure introduces some difficulties with the specification of the boundary conditions and is not especially well suited for flows with strong density gradients. The original version of the stream function-vorticity method reported in Ref. (1) used a point-by-point successive substitution procedure for the numerical solution of the equations and this procedure can allow only moderate nonuniformities in grid size (2). Indeed, large nonuniformity in the grid can lead to sufficient computational difficulty in the original stream function-vorticity method that the effects of different turbulent shear stress models cannot be ascertained (3). Later versions of the PISTEP programs have utilized line-by-line successive substitution methods which alleviate the non-uniform grid problem to some extent (2).

Despite the various problems that have been encountered in the use of the stream function-vorticity method it is among the most widely used techniques for the numerical solution of the elliptic governing equations. The problems involved with the approach have themselves led to the development of several closely related computational tools. One of the original applications of the stream function-vorticity approach was to the problem of the flow field within a sudden-expansion furnace configuration. El-Mahallawy et. al. (4) have reported a comparison of the results of such computations with

experimental data for a gas-fired furnace in which coaxial streams of fuel (central) and air (outer) enter a chamber through a sudden expansion. The method of Ref. 1 was used for these computations; it is not noted in Ref. 4 whether a point-by-point or line-by-line relaxation procedure was used. A very simple algebraic turbulence model is incorporated and the combustion process is approximated by a simple fully-reacted equilibrium model in which the fuel and oxidant are assumed to unite always in their stoichiometric proportions and intermediate species are ignored. Swirl could be induced in the experimental apparatus and the possibility of swirl was allowed for in writing the governing equations to be solved; however, it is not noted in Ref. 4 whether any nonisotropy in the eddy viscosity formulation in the swirling flow case was accounted for. The comparisons with experimental data reported in Ref. 4 show good agreement for centerline fuel mass fraction in the zero swirl case, fair agreement for spatial mixture fraction contours, again in the zero swirl case, and relatively poor agreement with flame length data for other than zero swirl. It is argued in Ref. 4 that the discrepancies with experimental data arise largely from the crude eddy viscosity model used.

Improvement of the turbulence model used to predict turbulent swirling flows with recirculation was one of the goals of the work reported by Roberts (5). In this investigation, limited to incompressible flow, the application of one member of the family of two-equation turbulence models developed by Spalding and co-workers to swirling pipe flow and swirling flow entering a sudden expansion was studied. Roberts found that in the case of swirling pipe flow, an anisotropic effective viscosity formulation in which the effective viscosity for axial momentum was obtained from the turbulence model and that for angular momentum from a mixing length model was satisfactory. However, for swirling flow entering a sudden expansion, he found that the ratio of the effective viscosity for axial momentum to that for angular momentum had to be as large as 40 to obtain good results, and furthermore that a constant eddy viscosity model produced much more satisfactory results than did the two-equation turbulence model in this case.

Roberts' comments with regard to the application of the stream function-vorticity model (1) to swirling flows with recirculation are of some interest. Roberts found that the numerical procedure of Ref. 1 was unstable for large swirl. This instability is caused by the source term in the vorticity equation which, for flows with swirl, includes a term involving the axial gradient of the square of the swirl velocity. At high swirl rates, when the computed flow field spreads rapidly, this term is very large, and if convective fluxes are low, it can dominate the vorticity equation. Since the vorticity is closely linked to the stream function, through the source term in the equation for the latter quantity, the result is that for swirling flows the computation involves three strongly coupled equations, one of which contains a large unstable source term.

The instability problem could not, Roberts found, be solved through the use of underrelaxation (the technique whereby only a fraction of the correction term calculated at one step is applied at the next step). Instead, a method referred to as MPCA (multipoint circulation adjustment) was developed to cope with the instability problem. In essence, MPCA requires that the distribution of stream function and vorticity always satisfies the circulation theorem. This method does not prevent overall change in the circulation around the entire flowfield; circulation changes at free surfaces and solid boundaries are still permitted.

While the MPCA technique apparently solved the instability problem encountered by Roberts (5), it creates severe difficulties in

overall convergence, increasing the time to obtain a converged solution by a factor of at least ten. Roberts explains this by noting that iteration procedures operate by sweeping imbalances, i.e. differences between the ultimate solution and the values held at any particular time in the computation, out to the edges of the computational field, where the boundary conditions correct them. The MPCA technique distributes the errors in all directions, including back into the computational field, greatly reducing the "correcting" influence of the boundary conditions.

An application of the PISTEP version of the stream-function-vorticity numerical technique developed by Gosman, et. al. (1) has been reported by Samuelson and Starkman (6) in the calculation of an opposed jet ammonia/air reacting flow field. As in the work of El-Mahallawy et. al. (4), a very simple algebraic eddy viscosity model is adopted, which for given inlet conditions, implies a turbulent viscosity that is simply proportional to the local density to the 2/3 power. The opposed jet flow field is one in which a jet of stoichiometric ammonia/air mixture is injected upstream along the axis of a ducted primary air flow. A large recirculation region is found as the jet stagnates and is turned to flow downstream and the flame is established by this flow process. In their calculation of this jet flowfield, Samuelson and Starkman utilized a highly non-uniform 15x33 node point grid, with a large number of node points clustered near the centerline and the jet nozzle. A simple global reaction model was used to compute the ammonia/air reaction progress. Comparison with experiment is presented for distributions of the fuel mole fraction and temperature. Calculations made assuming an adiabatic condition for the outer wall of the opposed jet do not agree well with experiment, while computations made assuming a constant wall temperature, extrapolated from the experimental flow field temperature data, show better agreement. However, in both cases the distribution of fuel mole fraction and temperature are incorrect in detail. Both Samuelson and Starkman (6) and El-Mahallawy et al. (4) state that the inadequacy of the simple turbulence model is probably responsible for the disagreement.

An application of the PISTEP code to the computation of the flowfield in a sudden expansion solid fuel ramjet combustion chamber has been reported by Netzer (8). In common with most applications of the PISTEP code, the application to the solid fuel ramjet has involved considerable modification, primarily to obtain numerical stability. Netzer has also incorporated a two-equation turbulence model in his formulation, as well as a method of treating the wall boundary condition which involves fuel regression and injection of mass into the flow field at the wall in this particular application. Netzer reports that the computation predicts a fuel rich recirculation region, an inlet flame pattern, and a distribution of turbulence intensity which are in good agreement with experiment, as are predictions of fuel regression rates and patterns as a function of air flow rate. However, diffusion rates in the boundary layer are predicted to be higher than experimentally observed.

A somewhat modified form of the original stream-function-vorticity computational technique described by Gosman, et. al. (1) has been used by Schulz in computations of a ducted, nonreacting, recirculating hydrogen-air flow (9). The configuration in this case involves a central stream of air or fuel and a secondary bleed flow through the wall of the sudden expansion at which the primary stream enters the mixing chamber.

Since there is insufficient mass in the secondary bleed flow to meet the entrainment needs of this primary jet, a large scale recirculation zone is set up around the central jet.

The intent of the investigation reported in Ref. 9 was to use the numerical procedure of Ref. 1 along with the results of variable-density recirculating - flow experiments to aid in the development of turbulence models for such flowfields. However, numerous problems were encountered which prevented this goal from being reached. Chief among these problems was an observed failure of the numerical procedure as applied to this flow field, to maintain a suitable level of mass conservation. One reason for this difficulty was the highly nonuniform grid that it was necessary to adopt in an attempt to adequately resolve the jet flow in a configuration in which the jet-to-duct diameter ratio was 10. It has already been noted in this discussion that the point-by-point relaxation technique incorporated in the basic version of the stream function-vorticity program is not well suited for highly nonuniform grids.

Perhaps the most extensive revision of the basic stream function-vorticity approach that has been reported is the field relaxation elliptic procedure (FREP) code developed by McDonald and co-workers (10,11). In this procedure the governing equations are written in the form used by Gosman, et. al. (1), but the FREP procedure uses an implicit computational scheme in which residuals are relaxed simultaneously throughout the entire flow field, rather than point-by-point or line-by-line. The intent of the code development has been to produce a technique directly applicable to realistic combustor geometries; it involves the time-averaged Navier-Stokes equations with coupled pseudo-finite rate chemical kinetics and a four-flux model for the computation of radiant heat transfer effects.

In most application of the FREP code reported to date, the effects of turbulence have been approximated through the use of an algebraic eddy viscosity model (an extended mixing length model) with a wall-flux model for the near wall region. Recent work using the FREP code has involved the incorporation of two-equation ($k-\epsilon$) turbulence model and a droplet burning and vaporization model (12).

The droplet vaporization and burning model used in FREP accounts for convection, diffusion, vaporization, and burning of droplets through a solution of the particle diffusion equations. The particle fraction is representative of the mass of liquid contained in an incremental droplet size range; five particle classes are assumed to represent a continuous range of droplet sizes. It is assumed that the droplets form a cloud of suspended particles, droplet/droplet interactions are neglected, droplet volume is very much less than the gas phase volume, and the droplet velocity is equal to the mean gas phase velocity. Further, the gas and liquid phase transport coefficients are equal. Single droplet theory is incorporated to account for the change of mass of droplets in a given particle class.

The pseudo finite-rate chemistry model involves the use of an equilibrium chemistry assumption for the hydrocarbon species and finite rate nitric oxide chemistry. This is a common assumption and provides a significant reduction in the amount of computer time required for a given calculation, but in general the NO_x formation reactions cannot be distinguished from, and are coupled with, the combustion reactions involving the exothermic

formation of CO_2 and H_2O (13). Other assumptions made in the application of the FREF code to the combustor flowfield problem include the use of the steady state Fick's law, which implies equal binary diffusion coefficients for each species in the mixture, unity Prandtl and Schmidt numbers, which eliminates a large portion of the complex source term in the total energy equation, and neglect of the contribution to the vorticity field which arises from the interaction of velocity gradient and the effective viscosity gradient.

In Ref. 10 the results of the application of the FREF code to swirling jet flows is described. It has been shown experimentally that such flowfields behave essentially as parabolic jets at low swirl rates, but at high swirl rates recirculation regions are encountered. Thus such flow fields provide a means of testing the predictions of the FREF code against relatively well understood and simple flow phenomena, and progressing from such tests to more complex flow fields. For these computations, a nonisotropic eddy viscosity distribution was used based on the extended mixing length model.

Specification of the appropriate initial and boundary conditions has been a major problem in the application of elliptic finite-difference techniques to the prediction of specific flows, and it is noted in Ref. 10 that the lack of detailed experimental inlet profiles precluded direct comparison of the predictions of the FREF program with experimental data, particularly in the small swirl case. Thus results are presented in similar coordinates, incorporating a virtual origin in the coordinate definition. Presented in this manner reasonably good results are obtained in the small swirl cases, although discrepancies are apparent in the computed and measured jet widths and velocity profile shapes. For the high swirl case, the initial centerline velocity decay rate is under-predicted, and again the velocity profile shape is not well represented.

Comparisons with data from both cold flow and hot flow sudden-expansion furnace experiments are also presented in Ref. 10. It is again noted in Ref. 10 that specification of the inlet and boundary conditions is a serious problem in the application of the elliptic method to these complex flow fields. For the cold flow case, the qualitative features of the flow field are observed to be well represented by the calculation, but a quantitative comparison shows some discrepancies, which are occasionally substantial. As in the jet case, the calculations at high swirl rates are observed to be substantially less affected by the inlet condition specification than those at low swirl rates.

Further difficulty was encountered in the calculation of the hot combustor flow field. Here there is some doubt as to the magnitude of the experimental swirl component, due to measurement difficulties in the reacting flow, compounding the problems involved in specification of the initial conditions. Comparison of the computed profiles of axial velocity, tangential velocity, temperature, and nitrogen oxide with experimental data shows only rough order-of-magnitude agreement with occasionally gross disagreement in details of the profile shapes. Predicted temperatures are found to be some hundreds of degrees higher than the measured temperatures; in part this can be attributed to the neglect of heat losses at the walls.

With the exception of the particular applications of the solid fuel ramjet and the opposed-jet configuration, the general experience with the stream function-vorticity method applied to combustor flows, as expressed

in the available literature appears to be that the method is capable of providing good qualitative flow field information but that attempts to obtain quantitative accuracy have generally not been successful. In part this situation may be due to the crudity of the turbulence models that have usually been used with the numerical procedure. However, attempts to use a more sophisticated turbulence model with stream-function vorticity approach have usually not been successful. An increased sensitivity to initial conditions, when a two equation model is used, has been noted in the development of the FREP code (12).

It is clear from the available work that the original code developed by Gosman, et. al. (1), incorporating a point-by-point successive substitution relaxation procedure should not be used for serious attempts to compute flow fields in which large scale grid nonuniformity is required for adequate resolution. The later developments of this code, which incorporate a line-by-line procedure, are apparently less sensitive in this respect, but the sensitivity of the formulation when large swirl rates are incorporated must be kept in mind. Spalding (2) has also noted that the stream function-vorticity method is not well adapted to flow phenomena in which large density gradients are encountered. Thus, it is somewhat questionable whether a stream function-vorticity formulation is an appropriate foundation for a general combustor calculation procedure. This is not to say that such a formulation cannot be made to work in specific cases; the work reported by Samuelson (6) and Netzer (8) and to a lesser extent the results of the use of the FREP procedure (10) indicate that good results can in fact be obtained, but it is apparent that the numerical problems involved with the stream function-vorticity approach are significant. Furthermore, the sensitivity of the method to the specification of initial and boundary conditions is quite severe (14,15); work is in progress to characterize and alleviate the boundary condition specification problem in the FREP code.

The problems encountered in the application of stream function-vorticity methods to variable density flows have led to interest in the application of methods which solve directly for the velocity components and the pressure. The application of such methods in the sudden expansion combustor problem is considered in the next section.

B. Pressure-Velocity Methods

Most of the recent computational work carried out at the Imperial College concerned with elliptic flow field problems has involved one or another of a family of codes which retain the pressure and velocity fields as the dependent variables. A general review of the computational approach used in the SIMPLE - Semi-Implicit Method for Pressure Linked Equation - code has been published by Patankar (16). As in the development of the stream function-vorticity approach, a standard form is used for the all of the time-dependent governing equations, which are then solved simultaneously. However, the simultaneous solution procedure cannot be used to obtain the pressure field. In the Imperial College approaches (such as TEACH, a simplified form of SIMPLE and the version of the code most readily available) an indirect method is used to obtain the pressure field.

The details of the numerical procedure used in the Imperial College pressure-velocity models may be found in Ref. 16. In summary, the solution procedure is as follows:

1. Provide initial estimates of the values of all variables, including an initial guess for the pressure P^* . Using the initial guess for the pressure, calculate auxiliary variables such as the density.

2. Solve the momentum equation to obtain a new velocity field with components U^* , V^* and W^* corresponding to the guessed pressure P^* at time $t_2 = t_1 + \Delta t$.
3. The true pressure P is assumed to be related to P^* by the expression

$$P = P^* + P'$$

where P' represents a pressure correction term. It is shown in Ref. 16 that the continuity equation can be used to generate a finite-difference equation for the determination of P' given the intermediate velocity components U^* , V^* , and W^* . This equation is solved to obtain P' at t_2 and thus the true pressure P .

4. Using the true pressure P , the true velocity components U , V and W are computed at $t_2 = t_1 + \Delta t$ using the momentum equation.
5. The true velocity components and pressure are used to solve the remaining equations relevant to a particular problem.
6. Returning to Step 1, the procedure is repeated for the next time increment. This is continued until the variables change little from step to step (if a steady state solution is desired) or until the desired final time is reached.

A number of applications of this procedure to problems similar to the sudden expansion combustor have been reported. Spalding has reviewed the application of the SIMPLE code and its derivatives to a number of problems such as a axisymmetric turbojet combustor (7). For this computation, a version of SIMPLE having the acronym EASI (elliptic axisymmetrical integration) is used along with a two-equation turbulence model, a transport equation for concentration fluctuations, a six-flux radiation transport model, and a simple equilibrium scheme for hydrocarbon kinetics, coupled with a NO_x kinetics formulation. Swirl is included. No results of computations with this approach are presented, although it is remarked that qualitative agreement with experiment has been obtained.

Patanekar and Spalding have also reported the development of an ambitious computer code for three-dimensional flows. An outline of one version of this code is described in Ref. 18, in which it is stated that the developed code will be applicable to steady, unsteady, laminar, or turbulent flow, with or without buoyancy, and with or without particle effects, and include either diffusion controlled or reaction limited chemistry, as well as convective, conductive, and radiative heat transfer effects. The numerical procedure (basically SIMPLE) is that which is described in Ref. 19 with "special tricks to reduce storage, increase speed and improve the ease and flexibility of boundary condition input." In Ref. 17 qualitative results are shown for the application of this code to the computation of a cylindrical fuel jet in a rectangular furnace. There is no comparison with experimental data.

The application of a similar model to a three-dimensional gas turbine combustion chamber problem is outlined in Ref. 20. This application involves the solution of the continuity, momentum, concentration, and energy equations, with a two-equation turbulence model, and a three-equation radiation heat transfer model. The radiation heat transfer model is developed from a six-flux representation of the radiative heat transfer. These fluxes represent the positive and negative elements of the components of radiation resolved in the three coordinate directions. The six distinct "bundles" of radiation are supposed to be representative of the whole radiative heat

transfer process. A uniform gas emissivity is assumed. Six first order differential equations can be written for the radiant energy fluxes. By combining the positive and negative fluxes along each coordinate direction, these equations can be converted into three second-order equations. The hydrocarbon reaction scheme involves a simple fully-reacted equilibrium model; the gas specific heat is assumed not to depend on composition or temperature.

For a three-dimensional recirculating combustor flow field, the numerical procedure is a version of SIMPLE called TRIC (three-dimensional recirculating flow in cartesian coordinates). There is also a polar-coordinate version known as TRIP. A very coarse $7 \times 7 \times 7$ grid is used, leading to a core storage requirement of 37K words on a CDC 6600, and 50 iterations require 60 seconds of CDC 6600 time. Only qualitative results are presented, i.e. computed profiles of longitudinal and cross-section velocity components, fuel mass fraction, temperature, and the radiative flux sums. No comparisons with experimental data is attempted, although it is observed that the results are qualitatively "real"

Recent work using the Imperial College TEACH algorithm has centered on the computation of two- and three-dimensional furnace flow-fields. Hutchinson, et. al. (21) present results of computations made for an axisymmetric, swirling, sudden-expansion combustor, including the effects of local fluctuations in species concentrations and of the density-velocity correlation terms in the governing equations. A two-equation turbulence model is used. The computations, which utilize a single-step, global hydrocarbon reaction rate expression modified to take into account the effects of local temperature and species concentration fluctuations (22), agree quite well with experimental data for mean axial and tangential velocity and mean temperature, centerline turbulence kinetic energy distributions and wall heat flux. It should be noted that the comparisons were made using a numerical code and experimental apparatus which were carefully made compatible, i.e., there were no features of the experimental apparatus which could not be included in the numerical model. Moreover, it is noted in Ref. 21 that the cost of the calculation was not negligible: a run time of 14 minutes on the CDC 6600 is quoted, using a 20×20 grid arrangement. Further, "familiarity with the detail of the computer program and skill in arranging the grid and under-relaxation parameters is also required."

A numerical code for three-dimensional elliptic furnace flows is described by Abou Ellail, et. al. (23). The numerical model is based on that reported by Patankar and Spalding (20) with "numerous refinements"; the physical models used include a two-equation turbulence model, a global fully-reacted equilibrium thermochemical model, a "six-flux" thermal radiation model, and a probability distribution function model for the influence of concentration fluctuations on the local mean temperature. Comparisons of predicted and measured axial mean velocity, temperature, and H_2O concentration are presented for a CH_4 -air furnace, as are horizontal and vertical profiles of temperature and velocity. The agreement is reasonably good, although some discrepancies thought to have been caused by differences between the actual experimental configuration and the computational analogue are observed. Of interest is the comment made in this paper that the solution to resolving the fine details of the flowfield appears to lie in performing separate, local calculations of zones in which fine detail is required and then using predicted conditions at the boundaries of these zones as input to the remainder of the calculation, which may then be performed on a much coarser grid than would otherwise be required.

Another group active in the development of numerical techniques suitable for solving the elliptic equations governing the flow in a sudden expansion combustor is that at the Los Alamos Scientific Laboratory (LASL). One of the techniques developed at LASA, the ICE (implicit continuous-fluid Eulerian) method reported by Harlow and Amsden (24,25) has been used as the numerical framework for the development of a numerical program for the computation of transient compressible laminar flow with multicomponent mixing and chemical reaction. This development, reported by Wieber (26), was primarily concerned with demonstration of the technique for computation of strongly coupled reacting flow in an axisymmetric geometry.

The ICE method is an implicit technique in which the pressure field at the advanced time step is obtained through the solution of a Poisson's equation. Somewhat like the SIMPLE code already described, the computation rests on the definition of a tentative pressure at the time step $t + \Delta t$.

The finite differencing with respect to time is written in a hybrid form with a parameter Θ ; such that for $\Theta = 1$, the expression is fully implicit, for $\Theta = 0$, it is fully explicit, and for $\Theta = 0.5$, the equation is time-centered. Central differences are used for the spatial derivatives, with all variables except velocity defined at the computational cell center, and the velocity defined on the cell boundaries. The sequence of operations in the solution procedure is as follows:

1. Given all data at the time step t , the Poisson's equation for the tentative pressure P at $t_2 = t_1 + \Delta t$ is solved, either through successive over-relaxation or the alternating-direction implicit (ADI) technique.
2. The new pressure \bar{P} is used to obtain the velocity components and density at t_2 . These are then used to determine whether the continuity equation is satisfied at time t_2 . If not, a new value of \bar{P} is computed, and the process is iterated until a suitable degree of convergence is obtained.
3. With the converged values of pressure, density and velocity at the time t_2 , the total energy and internal energy at t_2 are computed. If desired, the new internal energy may be used to recompute \bar{P} , and the entire iteration procedure repeated.
4. When satisfactory values of pressure, density, velocity, and total and internal energy have been obtained, the species equation is solved, taking into account both diffusion and chemical reaction. As is common in reacting flow solution procedures, the diffusion time step Δ is subdivided into a number of chemistry time steps to allow accurate computation of the progress of the chemical reactions in the flow.
5. After completion of the solution of the species equation, the equation of state is utilized to obtain the final value of the pressure at $t_2 = t_1 + \Delta t$. The procedure is then repeated until the desired final time is reached (for a transient computation) or until little change in the dependent variables is observed (for a steady state calculation).

As clear from even this brief summary, the application of the ICE method to the problem of transient, two dimensional compressible flow with chemical reactions is quite complex. By including a scheme for the point by point correction of the numerical diffusion errors caused by truncating the Taylor series during finite differencing, Wieber was able to obtain calculations of a wide variety of flows (26). These included flow startup in an infinite tube, shock tube flow, cyclical pulsation on a mean flow, uniform entry, coaxial entry into long and short tubes, flow of a center jet entering a sudden expansion,

and steady parabolic coaxial entry with mixing and chemical reaction of trace species. Wieber was not able to obtain successful computations of flows with strongly coupled chemical reactions, i.e. flows with large heat release, although he does recommend procedures to follow to improve the numerical capability in this case.

Of the work cited in this section, only the recent papers by Hutchinson, et. al. (21) and Abou Ellail et. al. (23) have reported successful comparison of calculation with experiment for recirculating flows with large heat release. Significantly, in both cases a careful adaptation of the numerical model to the specific experimental configuration was required, and both references note that the details of the computations require careful handling. It is clear that a considerable amount of development is required before the pressure-velocity approaches to the finite-difference solution of recirculating flows with chemical reaction lead to general and routinely usable techniques. On the other hand, these approaches do have intrinsic features which recommend their continued development. These include the ability of such techniques, at least in principle, to handle large density gradients, possible at the cost of a large number of grid points, and the relative ease and directness with which the boundary conditions in the problems may be specified. Furthermore, the recent work does show that successful computations of complex combustor flowfields can be carried out, and that the interaction of experiments and theoretical procedures designed for specific flowfields can provide considerable information to aid in the development of an accurate and general flowfield model.

C. Finite-Element Methods

An additional group of solution procedures applicable to the elliptic governing equations for a general combustor geometry is the finite-element methodology. Although the resultant finite-difference equations developed through use of this methodology are similar to those obtained with more conventional techniques, in principle, at least, the use of techniques such as the method of weighted residuals in deriving the finite-element equations yields a more flexible numerical approach. One of the more extensively reported finite element techniques applied to fluid dynamics problems is the COMOC code described by Baker and Zelazny (27). This code is designed for three-dimensional boundary layer type flows, and is hence parabolic; there is no fundamental difficulty in the application of the finite-element procedure to recirculating, and hence elliptic flows (28).

The application of the finite-element procedure to a ducted, three-dimensional, reacting hydrogen-air flow has been described by Zelazny, et. al. (19) and by Baker (30). For these computations the equation system involved the continuity, momentum, species, and energy equations. Most computations were carried out using a simple turbulent eddy viscosity model based on an extension of mixing length theory, although some calculations also were made with a two-equation turbulence model. The reaction chemistry based on a simple fully-reacted equilibrium approach for the hydrogen air system was used to model the primary effects of large heat release on the flow.

A number of comparisons of computational predictions with experiments are shown in Refs. 29 and 30; of most interest in this discussion is the prediction of the three-dimensional flow resulting from multiple round H_2 jets in a turbulent boundary layer. Good results for the downstream development

of hydrogen element mass fraction profiles are shown. The comparison of results obtained using mixing length theory and those obtained with a two-equation model of turbulence, shown in Ref. 29, indicates that the combination of the two equation model and a model for the turbulent Prandtl number can further improve the correlation.

This review of the applications of finite-difference and finite-element methods to the solution of the equations governing combustor flowfields with embedded recirculation zones indicates that there is as yet no method which has demonstrated an ability to compute the details of all of the physical processes which occur in a generalized combustor flow. A number of techniques are currently under development which show promise of becoming useful computational tools for this application, including, but not limited to, the FREP code, SIMPLE, ICE and the finite-element COMOC. Each of these methods has a special features of its own, as has been described in the preceding sections, but each also has its own difficulties. Because of the presumed intrinsic advantages of the pressure-velocity techniques with regard to applications to flows with large density variation and with regard to specifications of the boundary conditions, these types of numerical procedures appear to be preferable for the combustor problem; however, the pressure-velocity methods involve indirect and possibly time-consuming procedures to obtain the pressure field, and the relaxation techniques required in the solution procedure require careful handling.

The fully-implicit formulation used in both FREP and ICE is attractive from the standpoint of computational stability; however, such formulations of course involve considerably more computational complexity than explicit or semi-implicit methods such as SIMPLE and TEACH. Finite-element methods have not been applied to the same range of problems as have finite-difference approaches, particularly in elliptic flowfields, and thus it is difficult to assess their potential for combustor applications. However, it should be noted that the ease of specifying boundary conditions in a nonrectangular domain has long been considered a major feature of finite-element approaches, and this should carry over to elliptic applications as well.

The state of development of finite-difference (or finite-element) codes for the general combustor flowfield problem is such that they at present require rather severe simplification in the thermochemistry formulation in order to obtain solutions for specific flowfields with reasonable computer time, and it appears that there will be little change in this situation in the short term. This realization has led to the development of approximate techniques for dealing with combustor flow problems, and several types of approximate modular methods are described in the next section.

D. Approximate Methods (Modular Models)

The basic interest in the application of approximate techniques is to avoid the complexities inherent in a direct calculation of an elliptic flowfield by making suitable assumptions that allow the flow to be computed using simpler approaches. Clearly the simplest possible procedure is to assume that the flowfield is effectively one-dimensional thus avoiding any necessity for definition or calculation of velocity or species profile effects. A somewhat more sophisticated approach is to assume that the combustor flowfield can be broken down into separate zones, each of which can be calculated

individually in some detail, and then coupled together in some fashion to obtain an overall computational analog of the combustor flow. Such approaches are termed modular models, examples of which have been reported by Roberts, et. al. (31), Swithenbank, et. al. (32) and Edelman and Harsha (33).

The model described by Roberts et. al. (31) is a three-zone streamtube model, in which the flow in a gas-turbine combustor can be broken down into a primary zone (the central recirculation region), an outer streamtube of reacting flow surrounding the primary zone, and a single-streamtube dilution zone downstream of the primary zone in which the products of the outer streamtube are mixed with additional air and further reaction takes place. The model includes physical descriptions for fuel droplet burning and equilibrium or kinetic-limited hydrocarbon-air thermochemistry; the flows in each of the three zones are assumed to be one-dimensional. In all zones mixing of gaseous species is assumed instantaneous, while droplets in the streamline surrounding the recirculation zone are assumed to vaporize following a d^2 law; this vaporization rate governs the reaction rate in this zone. Gas phase chemistry is computed using a quasiglobal kinetics model following Ref. 34.

In the Roberts et. al. (31) modular model a key feature is the division of the mass flow entering the combustor into the rates feeding the three zones. The size of the primary, recirculation zone is obtained using an empirical relationship for recirculation zone boundaries in gas turbine combustion chambers. It is then assumed that air enters the recirculation zone only from the combustion air feed to the combustor can, at the downstream boundary, and the fraction of the total combustion air which enters the recirculation (the remainder flows into the dilution zone) is given by an empirical correlation. This air instantly mixes with the fuel in the primary region, and an equilibrium hydrocarbon combustion model is used, with finite-rate NO_x reactions proceeding for a residence time given by the volume of the recirculation region divided by the volumetric flow rate in this region. All fuel in this recirculation region is assumed to be in vapor phase, and the fraction of the total fuel flow in this region is given by the ratio of the recirculation region gas flow to the total flow (vapor and liquid phases) in the outer streamtube. The output from the recirculation region (equal to the input mass flow) mixes instantly with the unburned vapor phase fuel in the outer streamtube, initiating finite-rate reactions in this region.

This modular approach is obviously highly simplified and specialized to the gas turbine combustor. No direct comparison with data is given in Ref. 31, although it is noted that the prediction of absolute levels of NO_x at the combustor exit is good.

Because the elements of the modular model of Roberts, et. al. (31) are one-dimensional plug flow computations, conditions at the start of the calculation must be such that sustained combustion will be maintained. Such an initial assumption is not necessary when stirred reactor models are incorporated in the modular approach, as for example by Swithenbank et. al. (32). In this approach the combustor is modeled as a set of perfectly-stirred and plug flow reactors, arranged both in series and parallel. Here the perfectly-stirred reactors represent regions of intense recirculation. While this

approach will provide predictions of blowout phenomena and allow the use of arbitrary initial conditions, like the model of Roberts, et. al. (31) it rests on the ability to prescribe a priori the relative mass fluxes into each component of the model.

The modular approach described by Edelman and Harsha (33) is, like the model just described, an attempt to avoid some of the problems of elliptic flow field computation by devising an approximate treatment of a sudden-expansion combustor. There are however, significant differences in the assumptions made in the development of this modular approach compared to those involved in the model of Roberts et. al. (31), and these differences offer the potential for the former modular approach to handle considerably more complex problems than are possible with the latter technique.

In the modular approach of Edelman and Harsha (Ref. 33) the combustor flowfield is broken down into two major components: a directed flow, which is treated as parabolic, and a recirculation zone, assumed to be represented by well-stirred reactor(s). The two components are separated by a dividing streamline, whose shape must be specified a priori. Fluxes of species and energy across this dividing streamline form the boundary conditions on the two computational regions. Full finite-rate chemistry is included in both the directed flow and the well stirred reactor, and particle and drop-let effects can also be computed. The directed flow is assumed to be fully turbulent, except for the possible existence of a potential core along the flowfield centerline, and the shear stress distribution is obtained within this region through the use of a one-equation turbulence model (i.e. the turbulent kinetic energy equation with an algebraic specification of the dissipation length scale distribution).

Further details of the modular calculation approach can be found in Ref. 33. The method is currently in the developmental stage, but initial results have shown that the model provides at least a qualitative computational picture of a sudden-expansion combustor flowfield. The modular approach offers a technique and a tool for parametric investigation, which at least in the near term can include more of the physical phenomena involved in the sudden expansion combustor than can be easily accommodated in fully elliptic calculation procedures.

E. Summary of Required Work: Analytical Models

In view of the recent development in combustor modeling it is evident that substantial additional work is required to bring fully-elliptic finite difference (or finite element) methods to a point where they can be used productively in a more or less routine manner. It is also evident that more near term practical combustor modeling, as is of interest in the present program, can be achieved using a modular approach. Thus in order of priority the following modeling areas require further investigation:

1. Modular Modeling: The key element in the modular model of Ref. 33 is the shear layer model, which serves as a connecting link between the parabolic (directed flow) and stirred reactor (recirculation region) portions of the flow. Appropriate modeling for this region, in order to specify the

shear stress on the dividing streamline and the shear layer growth rate, both of which directly affect the transport of species across the shear layer and thus the feed rate to the stirred reactor model, requires further investigation.

2. Elliptic Formulations: Although elliptic formulations in principle provide a direct solution for combustor flowfields which involve extensive recirculation zones, there are severe numerical difficulties which limit the practicality of this approach. Thus further work is required with regard to boundary condition specification, grid arrangement, and other numerical details of the elliptic formulation.

II. TURBULENT FLOW MODELING AND THE PHENOMENON OF UNMIXEDNESS

In the last ten years there have been considerable advances made in the modeling of turbulent flows. Because of this work, it is now generally accepted that the turbulent kinetic energy models are the most appropriate for the computation of general turbulent flowfields, producing acceptable accuracy for engineering purposes in most flow fields of interest. The phenomenon of unmixedness, i.e., the apparent existence, in a highly turbulent flow, of regions in which both fuel and oxidizer can coexist, even with equilibrium chemistry, has also been a subject of much research interest and considerable advance.

A. Turbulent Kinetic Energy Model

The basic characteristic shared by all turbulent kinetic energy models is the use of the turbulent kinetic energy equation as a means of calculating the local turbulent shear stress field. Because the turbulent kinetic energy equation is a transport equation derived from the Navier-Stokes equation, models which use it to determine the local shear stress compute not only the local shear, but also its evolution as the flow field develops. Thus flow "history" is taken into account, and it is this feature that produces the great increase in generality that these models provide in comparison to the algebraic eddy viscosity models that have been commonly used in the past.

Since the application of turbulent kinetic energy models to flow fields of interest in combustor computations has been reviewed in detail elsewhere (35) this subject will not be discussed in detail here. For general reacting turbulent flows, which are of course of specific interest in combustor problems, two models have shown significant promise: the one-equation model developed by Harsha (36) and the two-equation model described by Rodi (37) and by Launder and Spalding (38). The basic differences between the two models lie in the relationship assumed between the turbulent shear stress and the turbulent kinetic energy and the formulation for the turbulent kinetic energy dissipation rate. In the one-equation model, the shear stress is assumed to be directly related to the turbulent kinetic energy, and the dissipation rate is calculated through the medium of a dissipation length scale, which is assumed to be algebraically related to the width of the mean flow field. The two-equation model, by contrast, involves an expression which relates the effective viscosity to the turbulent kinetic energy (a standard Boussinesq hypothesis is incorporated relating the shear stress to the effective viscosity) and an additional transport equation (also derived from the Navier-Stokes equation) is used to compute the turbulent kinetic energy dissipation

rate.

The application of both of these turbulence models to a reacting jet flow has been described by Edelman and Harsha (13); both are found to adequately represent the development of this turbulent flow field. Because of the relative simplicity of the length scale formulation in the one equation model, and the dominant effect of the dissipation rate term in the turbulent kinetic energy equation in most shear flows of engineering interest, modeling of this expression has produced good agreement with experimental data for a wide variety of high and low speed, reacting and non-reacting flows (36). On the other hand, the one-equation formulation can produce good results only when the relationship of the dissipation length scale to the mean flowfield width can be algebraically specified and this effectively limits the application of the one-equation model to parabolic flows.

Since the two-equation model includes a transport equation for the turbulent kinetic energy dissipation rate (or equivalently the turbulence length scale), it is well suited for the computation of elliptic flow fields in which the length scale cannot be specified as a function of the mean flowfield width. However, the turbulence modeling required for elliptic flows is incompletely understood, and far more experimental data providing experimental distributions of the turbulence correlations important in turbulence modeling in such flows is needed to adequately define the model in this case. The sensitivity of elliptic flowfield computations to the initial conditions specified in the calculations has been noted in the preceding sections. Specification of the initial distributions required for the turbulence model is clearly a further problem. A considerable amount of research on turbulence modeling in elliptic flows is presently being carried out however, and the development of appropriate models is unlikely to be a pacing item in the development of elliptic solution procedures.

B. Unmixedness

Although the time-dependent Navier-Stokes equations can in principle be used to describe in detail a turbulent flow, in practice this approach is not productive, except perhaps in extremely specialized and simple flows. This is true because no analytical solution of the general time-dependent Navier-Stokes equations, with time- and space-dependent boundary conditions exists, and recourse must in practice be made to numerical solution procedures. But in a turbulent flow the random fluctuations in the flowfield occur on a scale much smaller than can be resolved by the smallest conceivable grid*, and even if such spatial resolution were possible, the computation of the time-average quantities of engineering interest would

* An example, for computation of an axisymmetric pipe flow with $r = 0.5$ ft and $l = 2$ ft: Experiment shows that the smallest scales in which significant turbulence energy lies are on the order of 0.002 ft at $Re = 5 \times 10^7$ (39). Thus adequate resolution would require grid points spaced about 2×10^{-4} ft apart for a total of 2.5×10^9 grid points. Coarser spacing, i.e., at the smallest energy containing eddy size, would still require 2.5×10^5 grid points.

require N individual flowfield computations, each with different, randomly selected initial and boundary conditions, with N large enough so that a stable average is achieved. Thus recourse is usually made to the time-averaged equations of motion, which introduces two new problems: turbulence modeling and unmixedness.

The kinetic energy methods described above are one solution to the problem of turbulence modeling, i.e., writing expressions for the unknown quantities which appear in the time-averaged Navier-Stokes equations (see Hinze (39) for example) in terms of known quantities. However, the unmixedness problem still remains.

Consider a completely segregated flow consisting of equally sized eddies of material A and material B. A time-averaged measurement of this flow would show an average composition $c = (A+B)/2$. But in reality, no mixing on the molecular scale has taken place, and if A were fuel and B oxidizer, no reaction would have taken place. While complete segregation is never the case in a real turbulent flow, this example does point out that the time-average composition and the molecularly-mixed composition are not necessarily the same, yet it is the time-average composition which is computed from the governing species transport equation.

Methods for determining unmixedness are thus involved with the determination of the degree of molecular mixing which has taken place in a flow with a given time-average concentration. For flows in which finite-rate chemical reactions are taking place, an additional factor enters: because turbulence introduces random motions in all three coordinate directions, different eddies take different paths through the combustor, and thus even in a premixed flow there will be a spectrum of residence time. Further, in a flow which involves recirculation zones, backmixing of partially or wholly burned gases into the fuel-air mixture will also occur. Pratt (40) has reviewed the general subject of unmixedness, and he refers to the mixing of unreacted fuel and air streams as stream mixing, and the backmixing of partially or wholly burned reactants into the fuel-air mixture as age mixing. Then, for parabolic flows, only stream mixing need be considered (although there can still be a spectrum of residence times), while for premixed flows with recirculation zones, age mixing is the dominant mechanism. For nonpremixed flows with recirculation zones, which is of course the case in a general combustor, both stream mixing and age mixing occur.

In general, approaches to the unmixedness problem involve the definition of a probability density function for the combustion chamber variable for which unmixedness effects are to be investigated. For example, for elemental composition, C, $P(C)dC$ represents the fraction of the time interval Δt of the averaging process during which $C(t)$ is in the range $C_1 < C < C_1 + dC$. Then

$$\int_0^1 P(C)dC=1 \tag{1}$$

$$\bar{C} = \int_0^1 C P(C)dC \tag{2}$$

and the variance of the variable C is defined as

$$g^2 = \int_0^1 (C - \bar{C})^2 P(C) dC \quad (3)$$

For nonreacting flow, P(C) can be experimentally determined; for example, Rhodes (41) has shown that for shear layers the probability density function for concentration is well represented by a beta function, i.e.,

$$P(C) = (C)^{\alpha-1} (1-C)^{\lambda-1} / \int_0^1 C^{\alpha-1} (1-C)^{\lambda-1} dC \quad (4)$$

where

$$\alpha = \bar{C} \left[\bar{C} (1-\bar{C}) g^2 - 1 \right]$$

$$\lambda = (1-\bar{C}) \left[\bar{C} (1-\bar{C}) / g^2 - 1 \right]$$

Similarly, if $\alpha = t-t_0$ is the "age" of a given fluid particle, then it is possible to define the average "age" of particles in a combustor by

$$\bar{\alpha} = \frac{1}{T} \int_0^T \alpha P(\alpha) d\alpha \quad (5)$$

$$g^2 = \frac{1}{T} \int_0^T (\alpha - \bar{\alpha})^2 P(\alpha) d\alpha \quad (6)$$

where in this case, for random stochastic fluctuations,

$$P(\alpha) = \frac{1}{\sigma \sqrt{2\pi}} \exp\left(-\frac{(\alpha - \bar{\alpha})^2}{\sigma^2}\right) \quad (7)$$

The application of these concepts to the determination of unmixedness in combustor models of interest will be discussed in the following sections.

1. Stirred Reactor

In stirred reactor formulations, incoming (premixed or segregated) reactants are assumed to mix with products of reaction already existing within the reactor volume. For the computational limit of a perfectly-stirred reactor (PSR), this mixing is assumed to occur instantly and completely, forming a homogeneous mixture within the reactor volume, and chemical reaction takes place as bulk or volume burning. Numerous examples of PSR model formulations are available in the literature (e.g., Refs. 42-44). In addition to being a useful computational tool, in itself and as a model for the processes occurring in flowfield recirculation zones, such as behind a flameholder in a combustion chamber, well designed laboratory stirred reactors, such as that used in the experimental phase of this program, can approach the perfectly-stirred limit. Nevertheless, estimation of the effects of unmixedness are of importance in the use of analytical stirred reactor models, both in interpreting the results of stirred reactor experiments, particularly near blowout, and in developing stirred reactor formulations as components of analytical models such as the modular models described above.

A. Residence-Time Averaging

One approach to the computation of unmixedness in a stirred reactor is residence-time averaging, which considers the limit in which there is no mixing on the molecular level (45,46). The intense gross backmixing which occurs in a stirred reactor is simulated by dividing the entering reactant stream into a number of batches, or turbules, each of which is assumed to undergo one-dimensional batch reaction in the combustor for a different residence time, and then averaging the results using equation(5) with the well-known stirred reactor residence time distribution

$$P(t) = \frac{1}{\tau} \exp(-t/\tau) \quad (8)$$

as the weighting function. Thus, for each specie i

$$\bar{c}_i = \frac{1}{\tau} \int_0^{\infty} c_i(t) e^{-t/\tau} dt \quad (9)$$

When applied to the gas phase reactions in a stirred reactor this approach has the serious difficulty that the initial temperature must be high enough for one-dimensional reactions to proceed. Thus it cannot be used to study the phenomenon of blowout, since if the initial temperature is high enough for reactions to proceed there will always be some residence times included in the averaging which are sufficient to produce substantial reaction levels. Furthermore, since large molecular scale mixing is a key feature of the stirred reactor, a model in which the entering turbules remain completely segregated is a poor representation of the actual physical phenomena in a stirred reactor.

Residence-time averaging does have utility in the modeling of the physical phenomena in a two-phase stirred reactor system, as shown by Osgerby (47). The physical situation in this case is that even if the stirred reactor residence time is long enough for individual droplets to have evaporated following a d^2 law, the mixing process occurs in such a way that there will exist a distribution of droplet residence times and thus the mean liquid concentration in the reactor will be determined by the residence time distribution function. By postulating a model in which the gas phase is homogeneous, and chemically limited (i.e., molecular-scale mixing is instantaneous), and in which individual droplets do not interact, and are uniformly dispersed throughout the reactor, Osgerby obtains an expression for the mass fraction of droplets in the reactor as a function of time, t:

$$\frac{c_L}{c_{Lo}} = 2 e^{-d_o^2/\lambda\tau} \left[\sum_{n=0}^{n+1} \left\{ \frac{d_o^2}{\lambda\tau} \right\} \frac{1}{(5+2n)n!} \right] \quad (10)$$

where τ is the reactor residence time, d_o is the initial drop diameter, and λ is the evaporation rate constant, evaluated following Ref. 48.

B. The Two-Environment Model

A second approach to the problem of gas-phase unmixedness in a stirred reactor is the "two-environment" model proposed by Ng and Rippin (49). In this model, the physical phenomenon of unmixedness is modeled by assuming that the premixed reactants (the entering environment) enter as discrete batches or turbules, which then transfer to the leaving environment at a rate proportional to the mass remaining in the entering turbule. The proportionality constant is a mixing parameter, B, which can be related, at least approximately, to the turbulent intensity level in the combustor; B serves as a fitting parameter in the model. The outflow (leaving) environment from the reactor is taken to be a mixture of reactants, products, and reaction intermediates in a state of "maximum mixedness" as defined by Zwietering (50); this state is a function of the residence time distribution for the combustor system.

The two-environment model has been compared with experimental stirred reactor results by Bowman, et. al. (51); the analysis of Ng and Rippin (49) is shown in this paper to lead to the equation

$$\left(\frac{\dot{m}}{V_L}\right) [\sigma_i^{**} - \sigma_i^L] = r_i \quad (11)$$

in which V is the reactor volume, \dot{m} the mass flow rate, σ_i the mass concentration of species i (gmole i/gm mix), r_i the net reaction rate for species i, and the subscript and superscript L refer to evaluation in the leaving (outflow) environment. This is identical to the micromixed steady-state PSR equation, but with a fictitious feed-mass concentration given by

$$\sigma_i^{**} = [1 + (B/\alpha)] \int_0^\infty \sigma_i^e(t) \exp\left\{-\frac{t}{\tau}\right\} \frac{dt}{1 + (B/\alpha)} \quad (12)$$

where B is the mixing parameter, α is the reciprocal of the stirred reactor residence time, i.e., $1/\tau$, and $\sigma_i^e(t)$ indicates the concentration of species i at time t in the entering (i.e., unmixed) environment. When (B/α) equals zero (no molecular mixing), σ_i^{**} is simply the residence time-averaged concentration (equation (9)) for residence time τ ; for $(B/\alpha) \rightarrow \infty$ $\sigma_i^{**} \rightarrow \sigma_i^*$, where σ_i^* is the PSR inlet concentration and equation (11) reduces to the micromixed PSR equation.

Evaluation of equation (12) with an exponential (Arrhenius) formulation for $\sigma_i^e(t)$ (i.e., assuming one-dimensional batch reaction) is difficult, and Bowman et. al. (51) chose to assume that no chemical reaction occurs in the plug-flow (1-D batch reaction) portion of the model, thus $\sigma_i^e(t) = \text{constant}$ and

$$\sigma_i^* = \sigma_i^{**} = \sigma_i^e \quad (13)$$

Bowman, et. al. also note that the average value (averaged over entrance and leaving streams) for σ_i is given by

$$\bar{\sigma}_i = \frac{(B/\alpha)\sigma_i^L + \sigma_i^*}{1 + B/\alpha} \quad (14)$$

Since for a perfectly stirred reactor, $\bar{\sigma}_i = \sigma_i^L$, while for a plug flow reactor (with no reaction) $\bar{\sigma}_i = \sigma_i$, Equation (14) can be interpreted as expressing the average concentration of species i as a linear combination of well-stirred and plug flow reactor results.

The data that Bowman, et. al. compare the results of computations using Eqs. (11) and (12) with are O_2 consumption efficiency and NO concentration for subatmospheric stirred reactor operation, and they report that the two-environment model has utility only near blowout, at the lower pressure tested. However, it might be noted that the assumption of no reactions in the plug flow portion (i.e., a fraction of the total fuel is assumed to be essentially inert) would presumably be most accurate near blowout; further, there are sufficient areas of uncertainty in the prediction of NO reaction rates (and mechanisms) that comparisons with NO data may not be a true test of the model. On the other hand, Eq. (12) with a realistic reaction rate expression for $\sigma_i^e(t)$ is analytically intractable, and the basic assumption that a certain fraction of the stirred reactor does not mix with the remainder is certainly oversimplified.

C. The Coalescence and Dispersion Model

A model for the mixing of droplets in a chemical reactor has been proposed by Curl (52); this model can be equally well applied to gas-phase mixing by replacing the droplets in the model with "blobs" of gas. Basically, Curl's model assumes that initially segregated droplets (or "blobs") are fed continuously into a constant droplet population reactor, where randomly selected pairs of droplets coalesce, and after instantaneously mixing at the molecular level, re-disperse, so that the distribution of concentration among droplets is smeared or averaged out due to mixing. The concentration distribution is also altered by chemical reaction, through homogeneous batch kinetics during the time interval between blob or droplet encounters. Fresh material is fed in at a constant rate, and withdrawal takes a representative cut of the contents of the vessel.

Evangelista, et. al. (53) applied Curl's model to the study of unmixedness in a gas-phase stirred reactor, in which each blob behaves as a little batch reactor. They considered a single reaction where the concentration c of reagent behaves in batch according to

$$dc/dt = r(c) \tag{15}$$

and note that the contents of the reactor may be defined at time t by the concentration distribution $p(c,t)$ of particles at that time, where p is a probability density in c , with

$$\int_a^b p(c,t)dc \tag{16}$$

giving the proportion of particles having concentration between a and b at time t .

Curl (52) showed that the distribution of p satisfies the integro-

differential equation

$$\frac{\partial p(C,t)}{\partial t} + \frac{\partial}{\partial C} [r(C)p(C,t)] = \alpha \left\{ p_0(C,t) - p(C,t) \right\} + 2B \left\{ \iint p(C',t)p(C'',t) \delta \left[\frac{1}{2}(C'+C'') - C \right] dC' dC'' - p(C,t) \right\} \quad (17)$$

where $p_0(C,t)$ is the concentration distribution for the feed, $1/\alpha$ the nominal residence time of material in the tank and B a measure of the coalescence rate (mixing intensity). As in the two-environment model, B is a fit parameter whose value can be estimated empirically; Evangelista, et al. (53) give as an estimate for stirred reactors

$$B \approx 0.25 (L^2/A)^{2/3} \quad (18)$$

where L is a characteristic dimension of the reactor (diameter for a spherical reactor) and A is the total area of the injector jets.

The solution of Eq. 17 presents a formidable problem, even numerically, particularly if the reaction rate expression $r(c)$ takes on the Arrhenius form. Evangelista et al. concentrate attention on the late stages of reaction, where a polynomial (in conversion, x , rather the concentration, c) form for $r(c)$ may be assumed, and since they are concerned with high mixing rates obtain a first-order series expansion solution in powers of $1/B$, i.e.,

$$p(x) = p^{(0)}(x) + (\alpha/2B)p^{(1)}(x) + \dots \quad (19)$$

where $p^{(0)}(x)$ is the distribution in the ideally mixed limit $B \rightarrow \infty$. The solution is also considerably simplified by assuming a beta function distribution for $p(x,t)$, as in equation (4). The solution problem then becomes one of obtaining the mean and variance of the distribution.

The solutions obtained by Evangelista, et al. (53) are used to show the shift in the effective reaction-rate curve, and especially the reduction in the blowout limit, with decreasing mixing effectiveness. The results also indicate that the influence of unmixedness depends on the reaction kinetics: as m , the power of the polynomial conversion law, increases, the effect of variation in B/α increases, i.e., larger values of B/α are required to approach the well-stirred limit.

Although the governing equation for the coalescence-dispersion model can be written down (eq. 17), its intractability, particularly for realistic reaction rate expressions, and the fact that for multiple reactions a version of Eq. 17 must be solved for each species of interest limits its usefulness. This has led to interest in Monte Carlo simulation techniques for the unmixedness problem (43,54,55). The premise behind Monte Carlo simulation is that a suitable number of random samples of a stochastic process will eventually provide a result that is representative of the true average of the system. In this definition, the vague words "suitable," "eventually," and "representative" are used deliberately: the determination of the "suitable" number requires a number of simulations with different trial numbers,

"eventually" presumes that the simulation is convergent and will reach a steady state, and "representative" requires some knowledge of the true average. Monte-Carlo simulation is at best an approximate technique, and does not represent a means of obtaining a solution to Eq. 17 (although if the simulation is valid and Eq. 17 does represent the physics embodied in the model, the distribution obtained from the simulation should satisfy Eq. 17).

Spielman and Levenspiel (54) applied the Monte Carlo simulation technique to study the influence of coalescence on the progress of reactions occurring in the dispersed phase of two-phase systems in stirred reactors, i.e., to the droplet problem, while Kattan and Adler (55) studied gas-phase unmixedness in a tubular plug flow reactor with initially segregated components. The general application of the Monte Carlo technique to gas phase reactor calculations has also been reviewed by Pratt (43)

Conceptually, at least, the application of Monte Carlo simulation is simple. Following Pratt's outline (43), consider a steady flow reactor divided into K discrete segments $k = 1, 2, 3, \dots, K$ (see Fig. 1). The mass flow rate through the reactor is \dot{m} , and the total mass within the combustor is m . It is assumed that the total mass within the combustor at any moment, m , can be divided into N discrete "lumps" (or "blobs," or "turbules") of equal mass $m_k = m/n$. The total flow rate of these turbules is related to the mass flow rate:

$$\dot{N} = N \frac{\dot{m}}{m} = N \tau_s \quad (20)$$

where τ_s is the reactor residence time. Note that each discrete segment of the reactor consists of turbules which share a characteristic residence time

$$\tau_k = \left(\frac{k-K}{K}\right) \tau_s \quad (21)$$

Consider also two feeds (i.e., initially segregated) to the reactor, as shown in Fig. 1; the population, or number of turbules in feed 1 is N_1 , and that of feed 2 is N_2 . Then the feed rate of turbules is, from Eq. 20

$$\dot{N}_1 + \dot{N}_2 = \dot{N} = (N_1 + N_2) \frac{\dot{m}}{m}$$

so

$$\dot{N}_1 = N_1 \frac{\dot{m}}{m} = N_1 \tau_s \quad (22)$$

$$\dot{N}_2 = N_2 \tau_s$$

A calculation is started with an arbitrary distribution of turbules within the reactor volume. A discrete number of turbules from each feed stream, N_1/K and N_2/K are admitted into the combustor at cell

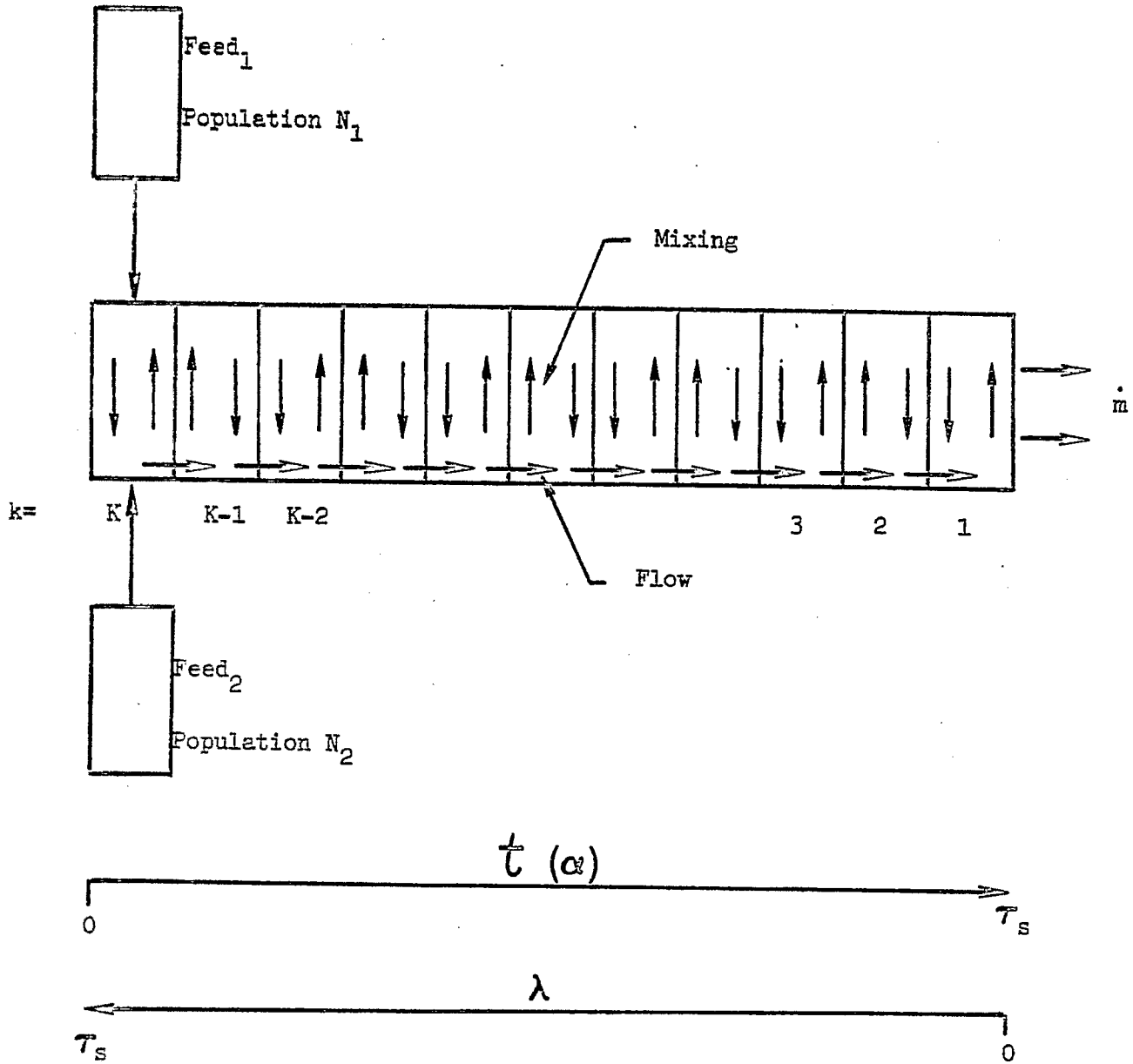


Figure 1. Monte Carlo Simulation

$k = K$ for which age $\alpha = \alpha_k = 0$ and residual lifetime $\lambda = \lambda_k = \tau - \alpha_k = \tau$; the population of the feeds is then replenished. The same number s of turbules, i.e., N/K , are displaced from cell k to cell $k-1$, and those from cell $k-1$ to cell $k-2$ etc; the turbulence in cell 1 exit from the reactor.

After this procedure takes place, a discrete number of pairs of turbules are selected for coalescence and dispersion, i.e., all conserved properties of the pair are averaged, and each member of the pair then assumes the average value just attained. The number of such encounters is given by

$$N_p = B(t)\Delta t N_K \quad (23)$$

where $B(t)$ is an empirical mixing frequency, $\Delta t = \tau/K$, and $N_K = N/K$. The determination of $B(t)$ is a key to the use of Monte-Carlo simulation; while $B(t)$ may be considered to be a fit parameter, it is also related to the turbulent intensity in the reactor and to the reactor geometry (see Eq. (18)). Empirical correlations for B of the form

$$B(t) = a + b \exp(-ct) \quad (24)$$

have been reported for plug flow combustors and diffusion flames, with $a = 40$ and $b = 300$ for plug flow (56) and $a = 60$ and $b = 300$ for diffusion flames (57).

With the mixing step outlined above completed, all turbules in each cell are allowed to undergo adiabatic batch reaction for the cell time increment $\Delta t = \tau/K$. The entire computation is then repeated until the outlet stream ($t = \tau_s$, $k = 0$) properties become time-stationary.

Excellent comparison of results of the Monte Carlo simulation with experimental data for a tubular, initially segregated, plug flow reactor has been reported by Kattan and Adler (55), using 300 cells; it is not noted how many repetitions of the simulation were required to reach a steady state. However, where application of the Monte-Carlo technique to a stirred reactor is concerned, the method just outlined has a serious flaw: mixing occurs only between turbules having identical ages. This flaw can be overcome, in principle at least, by allowing the feed population to contain a spectrum of ages given by an assumed distribution function for the specific reactor. Thus for a premixed stirred reactor one feed stream could be assumed to be entering reactants, all of age $\alpha=0$, while the other feed stream contains reaction products with a spectrum of ages. No results obtained using such a model have been reported.

2. Flowfield Unmixedness Models

Unmixedness models for flowing systems (i.e., two- or three-dimensional flowfields as distinguished from one-dimensional plug flow systems) fall into two major categories: probability distribution function models and correlation prediction models. In both cases, the ultimate goal is the same, to provide a means by which the instantaneous chemical reaction rate

can be obtained. Since in general the chemical reaction rate is a function of the local species concentrations and temperature, a method to obtain the instantaneous temperature and species concentration (as opposed to the time-average values of these quantities) is required.

If the flowfield is considered to be mixing limited, so that the chemical reactions can be assumed to be in equilibrium, the determination of the effects of fluctuations in temperature and species concentration is relatively simple. The solution of the transport equations for momentum, energy, and species yields the local average values of the velocity, enthalpy and species concentrations. The variance of scalar quantities in the flowfield can be related to the local turbulence intensity level (58) or obtained through the solution of a modeled transport equation (59). Then, a probability distribution function for, say, concentration of elements can be defined (e.g., equation 4). Thus the instantaneous element concentrations which contribute to the average at a point can be defined. Since equilibrium concentrations are functions both of the local element concentration and the local temperature, in general a joint probability distribution function of T (or h, the static enthalpy) and C should be used to obtain the local species distribution, but in most applications it is assumed that the enthalpy can be directly related to the element concentration. Thus a distribution of temperature is obtained and the local average temperature and thus density evaluated using the averaging rule (Eq. 2). A number of computations for various flowfields using this type of approach have been reported (e.g., Refs. 23, 58) with generally good results.

In situations in which mixing rates and chemical reaction rates are comparable, the problem of accurately assessing the influence of turbulent fluctuations becomes much more acute, because finite rate chemical kinetics is required. Then, a direct application of probability density function techniques would require the use of joint probability density functions for all of the active species, as well as the enthalpy. Even if such a joint PDF could be empirically determined, its use would still be computationally unwieldy.

One approach to the solution of the problem is the heuristic model of turbulent combustion proposed by Rhodes, et. al. (58). In this model, the flowfield is imagined as consisting of a large but finite number of zones and classes, where a class is all fluid anywhere in the flow whose elemental concentration C lies within ΔC on either side of a characteristic value, \bar{C} , and a zone is a region at a particular point in the flow whose average elemental concentration lies within ΔC on either side of \bar{C} . (In the work reported in Ref. 57 a hydrogen-air flame was considered, and so C was taken to be the elemental hydrogen concentration; in more complex chemical systems an overall stoichiometry variable could be used).

Given the definitions of classes and zones, the scalar probability density function P(C) is then the probability that a given class contributes to the average observed for a given zone. In order to carry out finite-rate chemical kinetics calculations, it is imagined in the Rhodes, et. al. (58) model that each class can be treated as a transient perfectly stirred reactor, that is, that for a molecular species in a class

$$\frac{d\bar{B}}{dt} = \bar{r}_B + \frac{d}{dt} \left(\bar{B}_f - \bar{B} \right) \quad (25)$$

Where \tilde{B} represents the mass fraction of a species in a given class. The following assumptions are made:

$$\frac{D\tilde{B}}{Dt} = U \frac{\partial \tilde{B}}{\partial x} \quad (26)$$

where U is the average velocity associated with the zone whose elemental concentration \bar{C} is the same as the class elemental concentration, \tilde{C} , and

$$\tilde{B}_f(\tilde{C}) = B(\bar{C}) \quad (27)$$

i.e., the chemical composition of the feed to class \tilde{C} is the same as the chemical composition of zone \bar{C} (in effect, it is assumed that the majority of the fluid making up class \tilde{C} is physically located in the flowfield region comprising zone \bar{C}). The chemical production rate \tilde{B} is obtained for each species from the usual kinetics appropriate to a homogeneous fluid, using the characteristic temperature and density for each class; the class total enthalpy is taken to be linearly related to the class elemental concentration.

It remains to define the term \tilde{m}_i/\tilde{m} for each species in each class. Because these terms computed for each species and each class must all be related, since overall mass and (in the absence of chemical reaction) individual species mass fractions must be conserved, a simple set of algebraic relationships can be derived to obtain the \tilde{m}_i/\tilde{m} (58). It is important to note that these relationships, which involve the probability density function for the appearance of class i in zone j replace the individual species conservation equations, i.e., the scalar probability density function provides the necessary information (along with the transport equation for elemental concentration) with which to compute the turbulent diffusion rate for each species. While this may at first appear to be a startling result, it might be noted that the scalar probability density function can be interpreted as a measure of the spread in a turbulent flow (caused by turbulent diffusion) of an initially localized scalar.

The major unresolved problem in this formulation is that it has been tacitly assumed that the degree of reaction is uniform for all fluid in a given class. While it is conceptually straightforward to imagine the classes broken down into subclasses by degree of reaction, this approach would introduce enormous complication. Moreover, there is no immediately observable a priori way to define the relative proportion of each subclass which contributes to a class, i.e., to define a probability density function for degree of reaction in a class. Given the assumption of uniform degree of reaction, quite good results were obtained using this model for a hydrogen-air diffusion flame (58); on the other hand this particular flowfield was relatively near chemical equilibrium, so that the assumption of uniform degree of reaction was relatively good.

The alternate approach to the computation of finite reaction rates in a reacting turbulent flow is to directly compute, through model transport equations, the additional correlations in the chemical production terms that arise when the variables are written in terms of mean and fluctuating parts and time-averaged (Reynolds averaged). Such an approach has been pursued by

Borghì (22) and by Bray and Moss (60), an example of computation using this approach is the recent work by Hutchinson, et. al. (21).

As noted earlier in part 1B of this section, the work of Hutchinson, et. al. involves a computation of an axisymmetric, swirling, recirculating, turbulent furnace flow. It is assumed that the chemical heat release can be modeled by a global, one-step finite rate chemical reaction, and the turbulent kinetics correction developed by Borghì (22) as modified by Khalil (61) is utilized. The solution procedure thus involves the solution of transport equations for the following quantities

- \bar{U} mean velocity component (x-direction)
- \bar{V} mean velocity component (y-direction)
- \bar{W} mean velocity component (z-direction)
- \bar{k} mean turbulent kinetic energy
- ϵ turbulent kinetic energy dissipation rate
- \bar{H} mean total enthalpy
- \bar{F} mixture fraction ($M_{fu} - \bar{M}_{ox}/i$) where i is the stoichiometric oxygen requirement by mass
- \bar{M}_{fu} mean fuel mass fraction
- $\overline{m_{fu}^2}$ mean square fuel mass fraction fluctuation
- $\overline{M_{fu} M_{ox}}$ fuel-oxidant mass fraction fluctuation correlation
- $\overline{\rho'u}$ density-axial velocity fluctuation correlation
- $\overline{\rho'V}$ density-radial velocity fluctuation correlation

and the fuel consumption rate is given by

$$R_{fu} = 10^{10} \bar{\rho}^2 \bar{M}_{ox} \bar{M}_{fu} \exp(-1.84 \times 10^4 / \bar{T}) \{1 + F\} \quad (28)$$

$$F = F(\bar{T}, \overline{T'^2}, \bar{M}_{ox}, \bar{M}_{fu}, \overline{M_{ox} T'}, \overline{M_{fu} T'}, \overline{M_{fu} M_{ox}})$$

It is noted in (21) that a probability distribution function was also utilized in this model for the evaluation of $(\bar{F}')^2$, i.e., fluctuation in the mixture fraction at a point, in order to allow the temporal (but not spatial) coexistence of fuel and oxidizer at a point. However, it is not clear from (21) how this model entered into the solution procedure, nor is it clear how the terms

$\overline{T'^2}$, $\overline{M_{ox} T'}$, $\overline{M_{fu} T'}$ which appear in the functional notation for F (Eq. 28) were evaluated:

Discounting the fluctuation terms just noted, the method of Ref. 21 involves the solution of twelve simultaneous transport equations, even for the simple global chemistry model used. Extension to more general chemical

systems would greatly increase this number, because of the additional cross-correlation terms that enter the problem; solution of a system of perhaps twenty to thirty simultaneous transport equations would represent no small feat, although it is not to be ruled out a priori. On the other hand, an observation made in the course of the work described in (58) may be relevant: it was found that the major heat-release reactions were relatively insensitive to turbulent fluctuation level (because for these reactions the reaction time was much less than the mixing time), while the reactions among trace species, such as NO_x , were quite sensitive. Thus, in specific situations it may be possible^x to limit the number of equations involved in a model such as Ref. 21 to a manageable number, while still obtaining a satisfactory estimation of the effects of turbulence.

C. Summary of Required Work: Unmixedness Models

The stirred reactor formulation is applicable to both the analysis of experimental data obtained in the course of this program and as a component of the modular combustor model, and description of unmixedness effects is important in both cases. The experimental stirred reactor used in this program has been shown to approach perfectly stirred conditions closely, and thus gas-phase unmixedness should not be important in the interpretation of experimental data. However, the analysis of residence time distribution effects on droplets and particles will be an important factor. Gas phase unmixedness effects will be potentially important in the use of the stirred reactor formulation as a component of the modular model. Further study of the unmixedness problem is required in all these areas, and priorities for this investigation can be set as follows:

1. Two-phase flows: The residence time distribution phenomenon requires further investigation with regard to the influence of droplet/particle coalescence or agglomeration on the predicted residence time distribution.
2. Gas-phase unmixedness: The two-environment model should be further investigated and compared with data that is less sensitive to unknowns in the chemical kinetics data than the NO formation data described above. However, this model does not allow any mixing to occur between reactant parcels of different ages, and so the Monte-Carlo approach should also be investigated as an aid in combustor model development.

Flowfield unmixedness effects also require further study for modeling combustor flows; here the spatial nonuniformity effectively rules out Monte-Carlo techniques and the near equivalence of reaction and mixing rates in some situations makes the use of probability distribution function techniques difficult. Further investigation of these models requires the following:

1. Correlation Techniques: Further work is required to model the correlations which enter the reaction rate expressions for turbulent flows, and to isolate those reactions which are, in a given system, most sensitive to the effects of turbulent fluctuations.
2. Probability distribution methods: In specific circumstances, i.e., rapid reactions or systems adequately described by global one-step reactions, these methods can provide accurate and useful results. Further work should center on the exploitation of these approaches where applicable, and on the development of methods to model the spatial distribution of state of reaction.

III. DROPLET AND SPRAY COMBUSTION

Many existing continuous combustions systems including aircraft gas turbines, furnaces, boilers and domestic heating units are designed to operate with direct liquid fuel injection. These systems have been designed and developed through an evolutionary process that has depended almost entirely on empirical information. Extrapolation to operating conditions other than the original design range has generally been met with serious problems. The situation becomes critical in terms of broadened fuel specifications required in order to provide economic and energy effective liquid fuels from coal and shale. In addition to the significant differences in H/C ratio, aromatic content and bound nitrogen levels of those liquids compared with petroleum based liquids the coal and shale derived liquids are more viscous and less volatile. While all these factors will affect the combustion process the higher viscosity and lower volatility have a direct effect on droplet size and spray dynamics. In order to establish the relationship between these fuel parameters and the combustion characteristics of these new liquid fuels models for spray dynamics and combustion are required. Although in dense regions of a spray droplet-droplet interactions are important the understanding of single droplet combustion is crucial to the description of the overall sprays. Furthermore, the basic mechanisms are similar for all fuels and consequently to establish the needs for further developments for new fuels the current state-of-the-art for more conventional fuels is relevant. The following discussions establish this need in terms of current droplet and spray modeling, respectively.

A. Droplet Modeling

To quantitatively describe the history of a vaporizing (or vaporizing and burning) droplet several mechanisms must be taken into account:

1. Conduction
2. Diffusion
3. Chemical and vaporization kinetics
4. Radiation
5. Convection

The description of each of these mechanisms varies in complexity as discussed below:

1. Conduction

When a small droplet or particle is initially subjected to a hot oxidizing environment it will begin to heat up due to conduction of energy from the surroundings. During this period, kinetics processes and species diffusion will be negligible and the heat-up process can be described simply in terms of the Fourier law of heat conduction. The droplet/particle size will either remain constant or increase due to a potential decrease in density.

2. Diffusion

During the initial heat-up period, the film about the droplet/particle will be uniform in composition being identical to that of the original environmental gas. However, as vaporization and/or surface reactions

start to prevail, concentration gradients develop and species diffusion will initiate. The diffusion of each species is relative to the mean convective flow where the environmental gases diffuse inward against the mean flow and the various species generated about the droplet/particle diffuse outward with a velocity equal to the combined diffusion velocity and mean outward convective velocity. The result is a non-uniform species field about the droplet/particle. Now, depending upon both the fuel/oxidizer and the associated temperature distributions, ignition will occur at some point and a flame may establish itself about the droplet/particle.

3. Chemical and Vaporization Kinetics

When chemical reactions enter the problem the need to distinguish between droplets and particles becomes crucial. Furthermore, the liquid droplets much also be classified according to whether they are pure or mixtures, light or heavy viscous liquids. As one spans the various types of liquids, the nature of the kinetic mechanisms changes. For example, pure hydrocarbon liquids readily vaporize and burn off completely with combustion occurring in the vapor phase about the droplet. Vapor phase cracking (pyrolysis) can occur in the hot fuel rich regions depending on how high the C/H ratio is (62). On the other end of the spectrum with heavy viscous liquids high temperatures are required for vaporization, with the attendant onset of surface reactions including liquid phase cracking and partial oxidation. Gas phase cracking and further oxidation subsequently occur off-surface around the droplet. Furthermore, the heavy liquids fractionally vaporize and this together with the cracking process can result in the formation of a residue. As the residue builds up a point is reached in the burning process where the rate of consumption is greatly reduced and a final stage of combustion involving the burn-off of residual coke-like particles is encountered (63). It is also noted that during the entire burning process the apparent density of the "remaining droplet" decreases with time which must also be accounted for in explaining the droplet time histories. For all fuel types, however, off-surface gas phase reactions generally occur.

4. Convection

Convective transport of mass and energy (and, in general, momentum) occurs when there is a relative velocity between the droplet/particle and the environmental gas. However, as the droplet/particle continues to heat up and vaporization and/or surface reactions become significant, the associated outward flow of "consumed" material establishes another mode of convective transport. Thus, once consumption processes have initiated, convection transport of mass and energy is occurring whether or not it is enhanced by the existence of relative motion.

5. Radiation

Although the relative importance of radiation heating compared with conductive or convective heating is small for single particles of practical size it must still be considered for purposes of experimental comparisons where generally larger droplets are used. Of course, the relative importance of radiation also depends upon the temperature levels of the surroundings but as pointed out by Hottel, (63), the dependence is primarily upon size. This is due to the dominant effect of heat transfer through

conduction from the flame for burning droplets. The situation is different in a spray where the heating of droplets of all sizes in the cool non-reacting core can be dominated by radiative heating from the flame structure in the outer regions of the spray. Whereas practical applications involve droplets of the order of 100 (μ) in diameter or smaller, experimental studies have involved substantially greater sizes ranging from the order of 1000 μ , (64), to 10,000 μ , (65). Thus to provide comparisons based upon existing and new data on large droplets and to provide a necessary ingredient for sprays in general radiation must be considered.

Although the coupling of these mechanisms to form a composite description of the single droplet consumption process is complex a vast amount of research and practical applications work has been done.

A review of the literature shows that liquid droplets have received most attention and pure metals next. While only few investigations have been reported on soot and various type carbon particle combustion these are significant in terms of the present investigation (see also Section II, Fuel Decomposition and Combustion). Much of the work on liquids has been done in non-burning configurations (66, 67, 68). These studies have relevance in terms of isolating vaporization times from the overall combustion process. Information of this type is most appropriate for applications where vaporization is essentially completed prior to ignition. These particular studies placed all the emphasis on the time required for consuming the droplets, so that detailed mechanistic studies were not essential and the data were generally correlated utilizing overall film coefficients. Detailed species histories were not relevant since it was tacitly assumed that the liquid simply transformed from liquid to vapor without any intervening chemical reaction. Nevertheless, a general conclusion was drawn from these studies; it was found that the following law applied:

$$d^2 = d_0^2 - \lambda t \quad (1)$$

where λ is the so-called "vaporization" constant, a function of the properties of the fuel and environment.

Perhaps one of the earliest mathematical treatments of the liquid droplet combustion problem was that of Godsave, (69). He assumed: (1) quasi-steady state, i.e., $\frac{\partial}{\partial t} \rightarrow 0$, (2) constant properties including droplet density, and (3) diffusion controlled combustion, wherein it is assumed that the droplet is surrounded by an infinitesimally thin flame surface at which combustion occurs instantaneously. The flame exists at the radial point where the fuel/oxidizer ratio is stoichiometric. The rate of vaporization is controlled by the diffusion of species to and from the flame surface and the rate of heat conducted from the flame to the droplet. The boundary condition at the surface was reduced to a simple balance between the heat conducted into the surface and the heat of vaporization. The droplet temperature was assumed constant at its normal boiling point. The result of the analysis included the derivation of the famous " d^2 -Law", i.e., Eq. 1.

Thus, even with the assumption cited above, the result was well-founded on the basis of experimental comparisons for light, pure hydrocarbons.

However, the details of the solution included temperature and species profiles, and, although limited to products of complete combustion, their rates of production were predicted. At about the same time period Spalding (64), has shown that for a variety of droplet and particle processes including vaporization and combustion, the "d²-Law" is appropriate. In general, this "Law" is indicative of the particular process being diffusion-controlled when kinetic rates are relatively fast. For example, Coffin and Brokaw (70), considered the "complete" combustion assumption and replaced it by a more general equilibrium model and, applying this to the Godsave formulation, essentially the same results were obtained. Even in Hottel's work on residual oils, (63) where he points out the need to consider additional effects including variable droplet density (as well as variable gas phase properties) the data yields linear relations between the 2/3 power of the instantaneous mass, m, vs. residence time. The basic result of Godsave is

$$\frac{dm}{dt} \sim d\lambda \quad (2)$$

where $m = \frac{\pi\delta d^3}{6}$; if δ (droplet bulk density) is constant the result is equivalent to Eq. 1. However, if δ is, in fact, not constant then Equation does not strictly apply unless some meaningful effective "constant" density could be assumed. If this were done and we let:

$$m = \pi \frac{\delta_{\text{eff.}} d^3}{6} \quad (3)$$

or

$$d = \left(\frac{6}{\pi\delta_{\text{eff.}}} \right)^{1/3} m^{1/3} \quad (4)$$

then

$$\frac{dm^{2/3}}{dt} \sim \left(\frac{1}{\delta_{\text{eff.}}} \right)^{1/3} \lambda \quad (5)$$

and in this form the result is much less sensitive to the density. The implication is that the primary controlling mechanism is the diffusion of mass and heat. Of course, the details of the ignition process, the formation of the residue (coke), and its ultimate disposition must include kinetics. Lorell, et al, (71) obtained numerical solutions to the droplet combustion problem with finite reaction rates. In this case, a one-step reaction was assumed to occur between fuel and oxidant to yield the product. Some years later, Peskin, et al, (72, 73, 74) treated the same problem with the introduction of a "modified flame surface" approximation that permitted exact solutions to be obtained. Here, the flame zone of finite thickness (due to finite rate reaction) is replaced mathematically by a Dirac delta-function centered about the flame surface. The results obtained indicated that for a wide range of fuel parameters and environmental conditions, an ignition-like phenomenon occurs as the ambient temperature is increased, which is marked by a sudden rise in the droplet burning rate. Similarly, an extinction phenomenon occurs as the ambient temperature is decreased.

Subsequently, Peskin, (75), obtained exact numerical solutions for comparison with the "modified flame surface" results and ascertained that the latter tended to predict ignition temperatures which were somewhat too

high.

The experimental work in (76), provides further evidence of the importance of kinetics on the ignition process and in the case of No. 6 fuel oil, surface reactions (pyrolysis) are important.

In the treatment of liquid fuel droplets, a number of studies have dealt with liquid mixtures (77). However, such mixtures are always treated as pure substances by assuming that they possess certain average transport and thermochemical properties. The bulk of the experimental liquid droplet combustion studies involve rocket motor applications wherein spray combustion is investigated in terms of combustion chamber performance rather than in terms of the detailed particle scale mechanisms.

It is apparent from the studies performed to date that a strong base exists from which practical single droplet models can be developed for the coal and shale liquids (77). However, special attention is required in the following areas:

1. Finite rate surface reactions.
2. Species evolution during droplet consumption.
3. Liquid and gas phase property variations.
4. Radiation in the case of large droplets, and for the interior droplets in sprays.

B. Spray Combustion

In order to achieve effective combustion of a liquid fuel it must be sufficiently dispersed to provide the large surface area needed for intimate contact with the air. This is generally achieved by injector configurations that atomize the liquid and produce a cloud of small droplets.

Although the single droplet combustion process is complex it is better understood than the spray combustion process. It appears that a major reason for this situation is that practical sprays are usually found in relatively complex turbulent flow fields involving non-uniform velocity, temperature and species fields. Furthermore, practical sprays involve a distribution of sizes affecting the aerodynamic and thermochemical properties of the spray. These factors are the main reasons for the difficulty in establishing the relationship between single droplet behavior and the combustion characteristic of a spray. Additional factors which set a spray apart from the single droplet configuration include the continuously changing environments about the droplets and droplet/droplet interactions which occur in dense regions of a spray. These effects tend to mask the underlying mechanisms controlling spray combustion characteristics and make the determination of the relationship between spray and single droplet combustion elusive. However, experimental observations made on uniform, monodisperse sprays (Ref. 78) have shown that " d^n "-Laws ($n \approx 2$) fit the overall spray consumption history but that the overall slope of d^2 vs. t is reduced from that given theoretically for single droplets. This result is extremely important in that it demonstrates the relevance of single droplet mechanisms to sprays. The reduction in consumption rate is not always observed, however, and in limited controlled experiments involving two burning droplets the burning rate first increased, reached a maximum and then decreased. This effect too can be explained in terms of single droplet mechanisms provided that the increase in gradients about a droplet and the decrease in oxygen concentration (as well as the changes in the

other environmental properties) are simultaneously taken into account. While the monodisperse spray experiments cited above show only a decrease in burning rate this observation is an overall one while in detail both effects are present. Since these processes are functions of size and number density of droplets in the spray a more general model and a wider data base is required before general conclusions can be reached. For coal and shale liquid droplets surface reactions including pyrolysis, partial oxidation and finite rate evaporation need to be investigated. The effect of these droplet surface processes will be to decrease the exponent in a " d^n "-Law such that if surface phenomena dominate, n will tend toward a value of unity.

In sprays ballistic transport for droplets with high momentum levels and diffusive transport for small, low momentum droplets, must be taken into account to properly describe the fuel distribution and droplet environment. The latter mechanism is relevant to most practical sprays where the droplets are transported mainly by the eddies in the gas phase matrix. Spray modeling in this context is discussed in general in Ref. (77). Specific applications which include provision for the mechanisms cited above are discussed in Refs. (79,80,81,82,83). These models are based on the continuum flow of each phase and account for the interphase transport of mass, energy, and momentum in turbulent polydisperse, two-phase diffusion flames.

In summary it appears at present that the development of droplet and spray models requires the following additional work:

1. Application and development of a practical droplet model which accounts for:
 - a. finite rate surface chemistry and vaporization
 - b. convective transport
 - c. radiation
2. Development of a spray model incorporating flow non-uniformities and turbulent transport processes applicable to modular modeling.
3. Application and development of a composite spray combustion model to new data covering ranges of conditions in uniform monodisperse dilute sprays and in dense sprays.

REFERENCES

1. Gosman, A. D., Pun, W. M., Runchal, A. K., Spalding, D. B. and Wolfshtein, M., "Heat and Mass Transfer in Recirculating Flows," Academic Press, 1969.
2. Spalding, D. B., "Turbulence Models and Their Experimental Verification, 3. Numerical Solution of the Differential Equation," Report HTS/73/18, Imperial College, April, 1973. (N74-12069).
3. Schulz, R. J., ARO, Inc., private communication, Dec. 1976.
4. El-Mahallawy, F. M., Lockwood, F. C. and Spalding, D. B., "An Experimental and Theoretical Study of the Turbulent Mixing in a Cylindrical, Gas-Fired Furnace," Combustion and Flame, Vol. 23, 1974, pp. 283-293.
5. Roberts, L. W., "Turbulent Swirling Flows with Recirculation," Report HB/73/3, Imperial College, January, 1973.
6. Samuelson, G. S. and Starkman, E. S., "Analytical and Experimental Investigation of an Ammonia/Air Opposed Reacting Jet," Combustion Science and Technology, Vol. 5, 1972, pp. 31-41.
7. Samuelson, G. S., "Mechanism of Exhaust Pollutant and Plume Formation in Continuous Combustion," presented at 1976 AFORS Contractors Meeting on Air-Breathing Combustion Dynamics, August 11-13, 1976, Air Force Aero-Propulsion Laboratory, Wright-Patterson AFB, OH.
8. Netzer, D. W., "Modeling Solid Ramjet Combustion," presented at 13th JANNAF Combustion Meeting, Naval Postgraduate School, Monterey, CA, 13-17 September 1976.
9. Schulz, R. J., "An Experimental and Theoretical Investigation of Confined Two-Stream Variable Density Turbulent Jet Mixing with Recirculation," Ph.D. Thesis, Univ. of Tennessee, June 1976.
10. Anasoulis, R. J. and McDonald, H., "A Study of Combustor Flow Computations and Comparison with Experiment," Report EPA-650/2-73-045, U.S. Environmental Protection Agency, December 1973.
11. Anasoulis, R. F., McDonald, H., and Buggelin, R. C., "Development of a Combustor Flow Analysis," Report AFAPL-TR-73-98, Air Force Aero Propulsion Laboratory, Wright-Patterson Air Force Base, January 1974.
12. Gibeling, H. J., McDonald, H., and Buggelin, R. C., "Combustion Modeling of Phenomena in Air Breathing Combustion Engines,; presented at 1976 AFOSR Contractors Meeting on Air Breathing Combustion Dynamics, August 11-13, 1976, Air Force Aero Propulsion Laboratory, Wright-Patterson AFB, OH.
13. Edelman, R. B. and Harsha, P. T., "Some Observations on Turbulent Mixing with Chemical Reactions," AIAA Paper 77-142, 15th AIAA Aerospace Sciences Meeting, January 1977.
14. Lanier, S., EPA, private communication, 1977.

15. Murthy, K., Purdue Univ., private communication, 1977
16. Patankar, S. V., "Numerical Prediction of Three-Dimensional Flows," in B. E. Launder, ed. "Studies in Convection," Academic Press, 1975, pp. 1-78.
17. Spalding, D. B., "Numerical Computation of Practical Combustion-Chamber Flows," Report HB/74/10, Imperial College, March 1974.
18. Patankar, S. V. and Spalding, D. B., "A Computer Model for Three-Dimensional Flow in Furnaces," HB/72/16, Imperial College, March 1972.
19. Patankar, S. B. and Spalding, D. B., "A Calculation Procedure for Heat, Mass and Momentum Transfer in Three-Dimensional Parabolic Flows," International Journal of Heat and Mass Transfer, Vol. 15, 1971, p. 1787.
20. Patankar, S. V. and Spalding, D. B., "Simultaneous Prediction of Flow Pattern and Radiation for Three-Dimensional Flames," HB/73/39, Imperial College, June 1973, also: Fourteenth Symposium (International) on Combustion, The Combustion Institute, 1974.
21. Hutchinson P., Khalil, E. E., and Whitelaw, J. H., "Measurement and Calculation of Furnace-Flow Properties," Journal of Energy, Vol. 1, No. 4, July-August 1977, pp. 212-219.
22. Borghi, R., "Chemical Reaction Calculation in Turbulent Flows Applicable to Co-Containing Turbojet Plume," Advances in Geophysics, Vol. 18, September 1974, p. 349.
23. Abou Ellai, M. M. M., Gosman, A. D., Lockwood, F. C., and Megahead, I. E. A., "Description and Validation of a Three-Deminsional Procedure for Combustion Chamber Flows," Report FS/77/27, Imperial College, Oct. 1977.
24. Harlow, F. H. and Amsden, A. A., "Numerical Calculation of Almost Incompressible Flow," Journal of Computational Physics, Vol. 3, 1968, pp. 80-93.
25. Harlow, F. H. and Amsden, A. A., "A Numerical Fluid Dynamics Calculation for All Flow Speeds," Journal of Computational Physics, Vol. 8, 1971, pp. 197-213.
26. Wieber, P. R., "Numerical Stuides of Unsteady Two-Deminsional Subsonic Flows Using the ICE Method," TM X-68288, NASA, August 1973, (N73-31240).
27. Baker, A. J. and Zelazny, S. W., "COMOC: Three-Dimensional Boundary Region Variant, Theoretical Manual and Users Guide," CR-132450, NASA, 1974.
28. Baker, A. J., University of Tennessee, Knoxville, TN, private communication.
29. Zelazny, S. W., Baker, A. J. and Rushmore, W. L., "Modeling of Three-Dimensional Mixing and Reacting Ducted Flows," AIAA Paper 76-49, January 1976, also Rushmore, W. L. and Zelazny, S. W., "Modeling of

Three-Dimensional Mixing and Reacting Ducted Flows," AIAA Journal, Vol. 14, No. 11, November 1976, pp. 1511-1512.

30. Baker, A. J., "Finite-Element Solution of Turbulent and Reacting Compressible Three-Dimensional Flows," Proceedings Second International Symposium on Finite Element Methods in Flow Problems, International Center for Computed Aided Design (ICCAD), Santa Margherita Ligure, Italy, June 14-18, 1976, pp. 609-620.
31. Roberts, R., Aceto, L. D., Kollrack, R., Teixeira, D. P., and Bonnell, J. M., "An Analytical Model for Nitric Oxide Formation in a Gas Turbine Combustor," AIAA Journal, Vol. 10, No. 6, June 1972, pp. 820-826.
32. Swithenbank, J., Poll, I., Vincent, M. W., and Wright, D. D., "Combustion Design Fundamentals," Fourteenth Symposium (International) on Combustion, The Combustion Institute, Pittsburgh, 1973, pp. 627-636.
33. Edelman, R. B. and Harsha, P. T., "AFOSR Interim Report on Mixing and Combustion in High Speed Air Flows," RDA-TR-0700-002, R&D Associates, Marina del Rey, CA, April 1976.
34. Edelman, R. B. and Fortune, O., "A Quasi-Global Chemical Kinetic Model for the Finite Rate Combustion of Hydrocarbon Fuels," AIAA Paper 69-86, 1969.
35. Harsha, P. T., "Kinetic Energy Methods," Chapter 8 of W. Frost and T. Moulden eds., Handbook of Turbulence, Plenum Press, 1977.
36. Harsha, P. T., "A General Analysis of Free Turbulent Mixing," TR-73-177, Arnold Engineering Development Center, 1974.
37. Rodi, W., "The Prediction of Free Turbulent Boundary Layers by Use of A Two-Equation Model of Turbulence," Ph.D Thesis, Imperial College, University of London, December 1972.
38. Launder, B. E. and Spalding, D. B., Lectures in Mathematical Models of Turbulence, Academic Press, 1972.
39. Hinze, J. C., Turbulence, McGraw-Hill, New York, 1959.
40. Pratt, D. T., "Mixing and Chemical Reaction in Continuous Combustion," Progress in Energy and Combustion Science, Vol. 1, No. 2/3, 1976, pp. 73-86.
41. Rhodes, R. P., "A Probability Distribution Function for Turbulent Flows," in Turbulent Mixing in Non-reactive and Reactive Flows, S.N.B. Murthy, ed., Plenum Press, New York, 1975, pp. 235-242.
42. Edelman, R. B. and Economos, C., "A Mathematical Model for Jet Engine Combustor Pollutant Emissions," AIAA Paper 71-714, 1971.
43. Pratt, D. T., Bowman, B. R., Robertus, R. J., and Crowe, C. T., "Comparison of Four Simple Models of Steady Flow Combustion of Pyrolyzed Methane and Air," Combustion Science and Technology,

Vol. 6, 1972, pp. 187-190.

44. Osgerby, I. T., "An Efficient Numerical Method for Stirred Reactor Calculations," AEDC-TR-72-164, AFOSR-TR-72-0410, Arnold Engineering Development Center, Nov. 1972.
45. Beer, J. M. and Lee, K. B., "The Effect of the Residence Time Distribution on the Performance and Efficiency of Combustors," Teenth Symposium (International) on Combustion, Pittsburgh, The Combustion Institute, 1965, pp. 1187-1202.
46. Fletcher, R. S. and Heywood, J. B., "A Model for Nitric Oxide Emissions from Gas Turbine Engines," AIAA Paper 71-123, 1971.
47. Osgerby, I. T., "Fuel Evaporation Rates in Intense Recirculation Zones," AIAA Journal, Vol. 13, No. 3, March 1975, pp. 394-395.
48. Mellor, A. M., "Current Kinetic Modeling Techniques for Continuous Flow Combustors," Emissions from Continuous Combustion Systems, edited by W. Coruelius and W. G. Agnew, Plenum Press, New York, 1972, p. 23.
49. Ng, D. Y. C. and Rippin D. W. T., "The Effect of Incomplete Mixing on Conversion in Homogeneous Reactions," Third European Symposium on Chemical Reaction Engineering, Pergamon Press, Oxford, 1964, p. 161.
50. Zwietering, Th. N., "The Degree of Mixing in Continuous Flow Systems," Chemical Engineering Science, Vol. 11, No. 1, 1959, pp. 1-5.
51. Bowman, B. R., Pratt, D. T. and Crowe, C. T., "Effects of Turbulent Mixing and Chemical Kinetics on Nitric Oxide Production in a Jet-Stirred Reactor," Fourteenth Symposium (International) on Combustion, The Combustion Institute, Pittsburgh, 1973, pp. 819-829.
52. Curl, R. L., "Dispersed Phase Mixing," AICHE Journal, Vol. 9, No. 2, 1963.
53. Evangelista, J. J., Shinnar, R., and Katz, S., "The Effects of Imperfect Mixing on Stirred Combustion Reactors," Twelfth Symposium (International) on Combustion, Pittsburgh, The Combustion Institute, 1969, pp. 901-912.
54. Spielman, L. A. and Levenspiel, O., "A Monte Carlo Treatment for Reacting and Coalescing Dispersed Phase Systems," Chemical Engineering Science, Vol. 20, 1965, pp. 247-254.
55. Kattan, A. and Adler, R. J., "A Stochastic Model for Homogeneous, Turbulent, Tubular Reactors," AICHE Journal, Vol. 13, May 1967, pp. 580-585.
56. Vassilatos, G. and Toor, H. L., "Second-Order Chemical Reactions in a Nonhomogeneous Turbulent Fluid," AICHE Journal, Vol. 11, No. 4 July, 1965, pp. 666-672.

57. Flagan, R. C. and Appleton, J. P., "A Stochastic Model of Turbulent Mixing with Chemical Reaction: Nitric Oxide Formation in a Plug Flow Burner," Combustion and Flame, Vol. 23, No. 2, 1974, pp. 249-267.
58. Rhodes, R. P., Harsha, P. T. and Peters C. E., "Turbulent Kinetic Energy Analyses of Hydrogen-Air Diffusion Flames," Acta Astronautica Vol. 1, 1974, pp. 443-470.
59. Spalding, D. B., "Concentration Fluctuations in a Round Turbulent Free Jet," Chemical Engineering Science, Vo. 26, 1971, pp. 95-107.
60. Bray, K. N. C. and Moss, J. B., "A Unified Statistical Model of the Premixed Turbulent Flame," AASU Report 335, University of Southampton, November 1974.
61. Khalil, E. E., "Flow and Combustion in Axisymmetric Furnaces," Ph.D. Thesis, Univ. of London, 1977.
62. Kobayasi, Kiyosi, "An Experimental Study on the Combustion of a Fuel Droplet," Fifth Symposium on Combustion, August 30-Sept. 3, 1954, pp. 141-148.
63. Hottel, H. C., Williams, G. C. and Simpson, H. C., "Combustion of Heavy Liquid Fuels," Fifth Symposium (International) on Combustion, 1954, pp. 101-129.
64. Spalding, D. B., "The Combustion of Liquid Fuels," Fourth Symposium (International) on Combustion, 1952, pp. 847-864.
65. Ranz, W. E. and Marshall, W. R., "Evaporation from Droplets," Chem. Eng. Prog., Vol. 48, 3 and 4, March and April 1952.
66. Foster, H. H. and Ingebo, R. D., "Evaporation of JP-5 Fuel Sprays in Air Streams," NACA RM E55K02, February, 1956.
67. Torda, T. P., and Matlosz, R., "Liquid Droplet Evaporation in Stagnant High Pressure and High Temperature Environment," NASA CR 72373, May 1968.
68. Eisenklam, P., Arunachalam, S. A. and Weston, J. A., "Evaporation Rates and Drag Resistance of Burning Drops," Eleventh Symposium (International) on Combustion, The Combustion Institute, Pittsburgh, 1976, pp. 715-728.
69. Godsave, G. A. E., "Studies of the Combustion of Drops in a Fuel Spray--The Burning of Single Drops of Fuel," Fourth Symposium (International) on Combustion, September 1-5, 1952, pp. 818-830.
70. Coffin, K. P. and Brokaw, R. S., NACA TN 3929, February 1957.
71. Lorell, L., et al, J. Chem. Phys., Vol 25, pp. 325-331 (1956).

72. Peskin, R. L. and Wise, H., AIAA Journal, Vol. 3, No. 9, pp. 1646-1650.
73. Peskin, R. L., et al, AIAA Journal Vol. 5, No. 12, pp. 2173-2178 (1967).
74. Polymeropoulos, C. E. and Peskin, R. L., "Theoretical Calculations of Fuel Drop Ignition and Extinction," Paper No. WSS/CI-76-5, presented at the 1967 Spring Meeting of the Western States Section/ The Combustion Institute.
75. Polymeropoulos, C. E. and Peskin, R. L., Combustion and Flame, Vol. 13, No. 2, pp. 166-172 (1969).
76. LeMott, S. R., Peskin, R. L. and Levine, D. G., "Effect of Fuel Molecular Weight on Particle Ignition," Combustion and Flame, Vol. 16, No. 1, February 1971.
77. Faeth, G. M., "Current Status of Droplet and Liquid Combustion," Presented at the 1977 Spring Technical Meeting, Central States Section/ The Combustion Institute, NASA Lewis Research Center, Cleveland, Ohio, March 28-29, 1977.
78. Beer, J. M. and Chigier, N. A., Combustion Aerodynamics, Halsted Press Division, John Wiley and Sons, Inc. 1972, pp. 179-184.
79. Edelman, R. and Economos, C., "A Mathematical Model for Jet Engine Combustor Pollutant Emissions," AIAA/SAE 7th Propulsion Conference, Salt Lake City, Utah, June 14-18, 1971.
80. Edelman, R., Economos, and Schmotolocha, S., "Analysis and Experiments on Multiphase Mixing and Combustion of Storable Fuels," 12th JANNAF Liquid Propulsion Meeting, Vol. I, p. 735, Las Vegas, Nevada, Nov. 1970.
81. Edelman, R. Boccio, J., and Economos, C., "An Analytical and Experimental Study of Some Problems in Two-Phase Flows Involving Mixing and Combustion with Applications to the B-O-H-N System," AIAA Journal, Vol. 9, No. 10, October 1971, p. 1935.
82. Edelman, R., Schmotolocha, S. and Slutsky, S., "Combustion of Liquid Hydrocarbons in a High-Speed Air Stream," (with S. Schmotolocha and S. Slutsky), AIAA Journal, Vol. 9, No. 7, July 1971, pp. 1357-1364.
83. Genovese, J., Edelman, R. and Fortune, O., "Some Aspects of Two-Phase Flows with Mixing and Combustion in Bounded and Unbounded Flows," (with J. Geneovese and O. Fortune), Journal of Spacecraft and Rockets, Vol. 8, No. 4, April 1971, p. 352.

IV. FUEL DECOMPOSITION AND COMBUSTION

The overall objective of this study is to describe the decomposition and oxidation of coal and shale derived hydrocarbon fuels using a quasi-global model.

The goal of this literature review on pyrolysis is to establish the global characteristics of the hydrocarbon decomposition with emphasis on soot formation. The mixtures described in this review are mainly fuel-rich gases, and the experimental results and theoretical computations reviewed here were obtained in the general range of 0.2 - 13 atm and 500 - 2700 K. In order to more easily delineate the main characteristics of the process, the review is presented in two parts, each being relevant to conditions in systems including gas turbines and other continuous flow combustion devices. These parts are: (I) fuel decomposition and (II) fuel oxidation.

A. FUEL DECOMPOSITION

The decomposition of the fuel is considered to be comprised of four major elements: pure pyrolysis, i.e., decomposition in the absence of oxygen; oxidative pyrolysis; soot formation; and soot oxidation.

1. Pyrolysis

To date the major fuels which have been studied are paraffins and olefins. For these fuels Chinitz (1) gives a global decomposition rate of the form

$$\frac{dC}{dt} = -kC \tag{1}$$

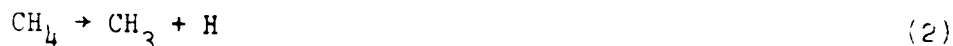
where C is the concentration in moles/cm³ and k is the first order rate constant for which the following values are available:

TABLE I

Hydrocarbon	Reference	k = A exp (-E/RT)	
		A Sec ⁻¹	E cal/mole
Methane	2	5.12x10 ¹⁴	101,000
	3	2.80x10 ¹⁶	107,600
Ethane	4	1.54x10 ¹⁴	70,200
Propane	1	6.3x10 ¹³	64,120

Equation (1) gives the global rate of disappearance of a general paraffin, C_nH_{2n+2}, but it does not provide information regarding the products of pyrolysis. A general survey of the literature reveals that in spite of

disagreements on the kinetic decomposition mechanisms for individual hydrocarbons, there is a consensus on the main products of pyrolysis. These are methane, ethane, ethylene and hydrogen. Experimental measurements on product-time histories for the major species produced during the pyrolysis of methane have been analyzed by Chen and Back (3). They were successful in predicting the early phases of the process but could not explain the plateau observed in ethane production. The rate-controlling reaction is thought to be

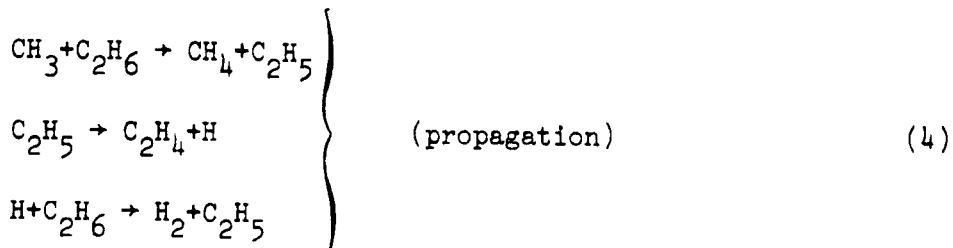
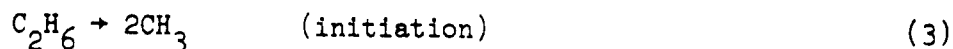


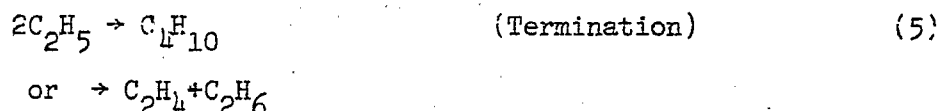
and the values of the Arrhenius parameters for this reaction are given in Table I. These rates are valid in the temperature range 1000 to 1400 °K. In contrast to the study of Reference 3, the work of Gardiner (5) is devoted to a study of methane pyrolysis in the high temperature regime encompassing the range of adiabatic flame temperatures from 2000 K to 2700 K at pressures ranging from 0.2 to 1.6 atm. Their suggested mechanism and rates is presented in Table II.

TABLE II

Reaction	Rate constant cm ³ /mole sec
$\text{CH}_4 + \text{M} \rightleftharpoons \text{CH}_3 + \text{H} + \text{M}$	$2.3 \times 10^{14} \exp(-64.5 \times 10^3 \text{ cal/RT})$
$\text{H} + \text{CH}_4 \rightleftharpoons \text{CH}_3 + \text{H}_2$	$2.2 \times 10^4 \exp(-8.84 \times 10^3 \text{ cal/RT})$
$\text{CH}_3 + \text{CH}_3 \rightleftharpoons \text{C}_2\text{H}_4 + \text{H}_2$	$6.0 \times 10^{16} \exp(-43 \times 10^3 \text{ cal/RT})$
$\text{CH}_3 + \text{CH}_3 \rightleftharpoons \text{C}_2\text{H}_6$	8.43×10^{12}
$\text{C}_2\text{H}_4 + \text{M} \rightleftharpoons \text{C}_2\text{H}_2 + \text{H}_2 + \text{M}$	$10^{14} \exp(-49.93 \times 10^3 \text{ cal/RT})$
$\text{H}_2 + \text{M} \rightleftharpoons \text{H} + \text{H} + \text{M}$	$2.23 \times 10^{12} \text{ T}^{1/2} \exp(-92.45 \times 10^3 \text{ cal/RT})$
$\text{CH}_3 + \text{CH}_3 \rightleftharpoons \text{C}_2\text{H}_5 + \text{H}$	$4.0 \times 10^{14} \exp(-17.92 \times 10^3 \text{ cal/RT})$

The kinetic mechanism for ethane is generally agreed (6) to be:





The value of the Arrhenius parameters of the controlling initiation reaction is given in the following table

TABLE III

Temperature Range °K	Reference	Log $\frac{A}{\text{sec}^{-1}}$	E , kcal/mole
837-881	7	17.45	91.7
748-873	8	14.50	81.0
823-893	9,10	16.00	86.0
839-873	11	16.30	88.0
948-1048	12	16.30	86.0
-	13,14	14.80	71.8
898-1048	15	16.36	87.0

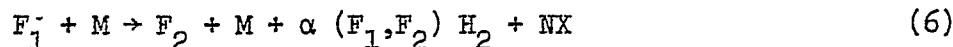
Chinitz (1) points out that the disappearance of butane is first order with respect to C_4H_{10} , and that the rate constant may be expected to be close to that of propane.

A survey of the literature on the kinetic mechanism of decomposition of olefins shows that the situation is much less clear than for paraffins.

Studies for ethylene (Ref. 16 in the range 0.2 - 0.8 atm and 773-875 °K and Ref. 17 in the range 0.01 - 0.35 atm and 798 - 923 °K), for propylene (Ref. 18 in the range 800 - 900 °K) and for isobutene (Ref. 19 in the range 770 - 870 °K at 1 atm) present only qualitative results, but no quantitative information is given.

The fuels which are relevant to our study are coal and shale liquids and gases characterized by a low H/C ratio, high aromatic content, high bound nitrogen and high viscosity for the liquids. Thus, information on pyrolysis of aromatics is most relevant here. The status of the knowledge on the subject was recently summarized by Golden (20). The conclusion was that there is a dearth of information on the subject.

However, because of the observation that there is a commonality of major pyrolysis products for all studied hydrocarbons, we can reasonably assume that a global reaction of the type



which is valid for paraffins, can be also expected for aromatics if F_2 is chosen to be one of the major known products of hydrocarbon pyrolysis. In Equation 6, F_1 represents the original fuel, M a third body, α can be 0

or 1 depending upon F_1 and the choice of F_2 , and NX is the "model" nitrogen bearing compound after Caretto (21). Following Chinitz (1), we can write the rate of disappearance of F_1 as

$$\frac{dC_{F_1}}{dt} = - A_1 C_{F_1} \exp(-E_1/RT) \quad (7)$$

where A_1 and E_1 will have to be determined from experimental data obtained in this program using the well-stirred reactor.

2. Oxidative Pyrolysis

Since pyrolysis occurs in the presence of oxygen, it is necessary to establish the effect of oxygen on the thermal decomposition process.

Bradley and Durden (22) studied the high temperature (1200-1600 K) reactions of propane, propylene, propane and oxygen, and propylene and oxygen. The authors noticed that while the relative amounts of reaction products varied with temperature, they showed no dependence on the oxygen concentration; no oxygenated products apart from carbon dioxide were ever observed. These observations were valid for both small (C_3H_6 - 0.6%, O_2 - 0.2%) and large (C_3H_6 - 0.6%, O_2 - 2.9%) quantities of oxygen mixed with fuel and a large amount of inert gas. As the amount of oxygen added to the mixture increased, the overall rate of reaction increased as well, but only slightly. These results were explained by the fact that at the high temperatures used here, pyrolysis is dominated by the rate of the initiation reaction which is "catalyzed" by oxygen, while direct reactions between the products of pyrolysis and oxygen occur only on a large time scale.

Murgulescu and Bicã (19) confirmed the above observation by studying the pyrolysis and oxidative pyrolysis of isobutene at atmospheric pressure and 775 - 875 K. Further, the authors show that the activation energy for oxidative pyrolysis is 24.9 kcal/mole, which is significantly smaller than the value of 48 kcal/mole (815 - 873 °K) attributed to the pure pyrolysis reaction (23, 24). This is in direct agreement with the observation that oxygen enhances thermal decomposition. A lowering of the activation energy of the reaction when oxygen is present had also been previously observed for both ethylbenzene (25) (48.5 kcal/mole compared to 70 kcal/mole) and n-butane (26) (21 kcal/mole compared to 61.4 - 73.9 kcal/mole).

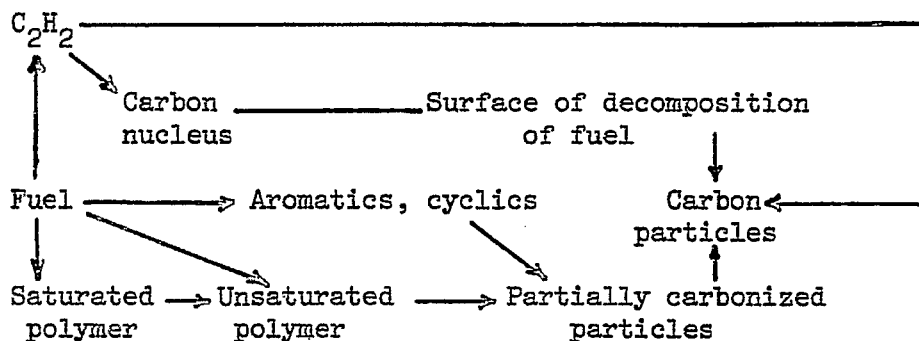
From the point of view of our model, it is important to establish the variation of the activation energy, E_1 , in Equation 7, and possibly A_1 (although it is not mentioned in any of the above studies), with the oxygen concentration in the mixture. This information is not yet available in the literature, and should come out of experimental results on pyrolysis in well-stirred reactors.

3. Soot Formation

Soot forms during pyrolysis of hydrocarbons and as the H/C ratio of the pyrolysing hydrocarbon becomes small. Soot production increases.

The formation of soot is a complex process sensitive to many properties of the flow including composition, temperature and the presence of surfaces. Because of this, and the difficulty in separating the physical (nucleation, coagulation and growth) and chemical (kinetic mechanisms) features of soot formation, definitive experiments on the mechanism of soot formation are yet to be done. In spite of the lack of detailed understanding of the soot formation process, there is evidence that suggests that global formation rates can be defined in terms of other measurable properties of the reacting flow.

In their review of soot formation from gases, Palmer and Cullis (27) point out that there are at least eight theories of soot formation, each theory being more qualitative than quantitative. There is a "C₂ theory" (28) suggesting that solid carbon forms by polymerization of C₂, an "atomic carbon theory" (29) which views monoatomic carbon as a possibly significant species in nucleation, and the theory of Cabannes (30) which advocates that solid carbon forms by condensation of carbon vapor the main constituent of which is C₃. Other theories (31,32,33) support the view that carbon particles are formed by simultaneous polymerization and dehydrogenation of acetylene. Street and Thomas (34) suggest that the fuel is first polymerized and then dehydrogenized, oxidation possibly aiding both processes, and that carbon is the end product of this sequence. The following scheme, reproduced from Reference (34) summarizes the path of soot formation according to Street and Thomas.



Other studies (35) claim that decomposition of hydrocarbons at the carbon particle surface is responsible for the particle growth. Finally, there are other theories (36,37) suggesting that carbon is formed in premixed flames through the reaction $2 \text{CO} \rightleftharpoons \text{CO}_2 + \text{C}_s$.

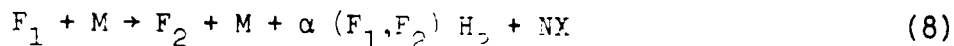
For purposes of interpreting experimental results performed with the well-stirred reactor, the conclusion of studies regarding the soot formation in premixed flames (soot formation depends on the flow properties, and thus the process can be different in diffusion flames (38)) is most relevant. There are several well-established facts about the overall chemistry of soot formation: (1) it is a nonequilibrium process (39) (thermodynamic equilibrium requires a C/O ratio of unity, but in fact this ratio is smaller - about 0.475 for n-paraffins and 0.83 for acetylene), (2) the threshold mixture at which carbon starts appearing is quite insensitive to back-mixing (40), (3) the essential carbon-forming process does not involve ring rupture of aromatics to smaller fragments (41) and while benzene rings favor soot formation, hydrogen and excess oxygen act as inhibitors (42), (4) the unreactive p.c.a.h's are by-products of soot formation and soot formed from the reactive p.c.a.h's accounts only for a small fraction of the total soot yield in flames (43), and (5) acetylene is a soot precursor (44). We notice again that all this information is qualitative rather than quantitative and that there are no global rates of soot formation available in the literature.

However, there are important conclusions in the above statements with respect to our global model: (1) we need a kinetic model to describe soot formation, (2) we can safely not account for the p.c.a.h's and (3) acetylene should play a definite role.

Measurements of soot particle-size have established that while the mean size of those particles is about 250 Å (45), particles as small as 50 Å (44) and as large as 6000 Å (39) have been observed. The origin of the nuclei which are the basis of the soot particles is yet unclear; ions have been proposed (46,47,48,49,50) but it was also pointed out that large hydrocarbon radicals rather than ions are more likely to be nuclei for soot forming in a premixed flame (51); dust particles and small molecules containing a few carbon atoms have also been suggested (52).

By using ions as nuclei and kinetic models of varying sophistication to describe the physical processes of nucleation, coagulation and growth of particles, Howard and his coworkers (46, 47, 48, 49, 50) showed that the nucleation rate is high in the early part of the flame and goes to zero in the burned gases. This means that the particle number concentration is governed initially by nucleation and later by coagulation. Surface growth rate dominates the rate of mass addition but was found to play a secondary role to coagulation in governing the increase in particle size. There is at least one study (52) which shows that observable quantities, such as soot concentration and number of soot particles of each size do not depend on the origin of the initial nuclei; but it was also recognized that this conclusion may not be valid in all situations. The study of Jensen (52) is unique among investigations on soot formation, in that it presents a unified model which reconciles chemical and physical features of the process. All five basic mechanisms involved in the process of soot formation at a temperature above 1000 °K, namely, gas reactions producing radical fragments on which nucleation begins, nucleation, coagulation, growth and oxidation, were taken into account. In this model both chemical reactions yielding fuel decomposition products, and growth of particles from small to larger sizes (particles of same radius are treated as a particular species) proceed at kinetic rates similar to the Arrhenius law. This model was successfully applied by Jensen (52) to the non-equilibrium conditions in the chambers of rocket motors (using the liquid propellant isopropyl nitrate) in order to predict whether or not the exhaust of such motors will be smoky. The author cautioned against extrapolation of his model for cases where the kinetic rates for coagulation of the larger particles happened to play an important role in determining the overall rate of conversion of the fuel (methane in his case) to soot and H₂.

For our modeling purpose, Jensen's study has interesting potentials. Since it was recognized that soot appearance lags behind that of other products of pyrolysis (see Fig. (1) and recall that acetylene is a soot precursor), one could think of representing soot formation by the following sub-global scheme



where F₁ is the original fuel, F₂ is a lower molecular weight hydrocarbon (a major product of pyrolysis), M is a third body, C_s represents the soot,

α can be 0 or 1 depending on the H/C ratio, of F_1 and the choice of F_2 , and NX represents the decomposition result of the nitrate bound in the fuel. If we chose F_2 to be CH_4 , we could use Jensen's model and rates to predict soot formation.

We note, however, that a global rate of the type needed for the second reaction of the above scheme is not yet available. The two parameters needed are A_2 and E_2 in the expression

$$\frac{dC_{F_2}}{dt} = - A_2 C_{F_2} \exp(-E_2/RT) \quad (10)$$

This new information will be obtained as part of the experimental program to be conducted using the well-stirred reactor.

4. Soot Oxidation

Table IV gives an indication of the information which is available in the literature on soot oxidation. For a long time the study of Lee, Thring, and Beér (53) was the only comprehensive study of soot combustion. It was found in this study that in a laminar diffusion flame, under the physical condition shown in Table IV, the combustion rate of soot particles is chemically controlled. The rate was related to the flow conditions through the expression

$$K_s = \frac{\rho d_0}{6 m_0} \frac{1/3}{m} \frac{2/3}{P_{O_2}} \frac{dm}{dt} \quad (11)$$

where ρ is the density of soot, d_0 is the initial diameter of the particles, m_0 is the initial mass flow, m is the instantaneous mass flow and p_{O_2} is the

partial pressure of oxygen. Khan, Wang and Langridge (54) used the same expression as the authors of Ref. (53), but found in their experiments rates somewhat higher than those of Lee, Thring and Beér (53). The Arrhenius parameters of Ref. (54) are also presented in Table IV. In contrast to Lee, Thring and Beér (53), Parker and Hottel (55) made measurements for large carbon spheres and found that for those large particles combustion was diffusion controlled. The results of Field et.al., (56) were also obtained for carbon particles (coal and charcoal) and for this reason it is thought that their rates were also much higher than those obtained for soot. In Table IV there is a comparison of the Arrhenius parameters given by the authors of Refs. (53, 55, 56). By far the most complete study of soot oxidation existing to date is that of Park and Appleton (16). Their experimental results show that for a fixed oxygen partial pressure the reaction rate increases with temperature up to a local maximum; as the temperature is further increased a minimum is obtained and the rate again increases with temperature. This is illustrated in Fig. 2 reproduced from Ref. (57). Shown on the same graph are the results of other investigators, (53, 58, 59) and the curves represent theoretical calculations using the formula of Nagle and Strickland - Constable (60) given in Table IV. The results of Fig. 3 show further that when the temperature is fixed (≈ 2500 °K) and the oxygen partial pressure is small ($p_{O_2} < 0.1$ atm) the reaction rate is proportional to the oxygen concentration, in agreement with the results of

Ref. (53); however, as the oxygen partial pressure increases ($p_{O_2} \geq 1$ atm) the rate approaches an asymptotic limit, i.e., there is no dependence upon the oxygen concentration.

Thus, if soot oxidation is represented by the reaction



we have two choices at present on how to model the rate of the reaction. One choice is to use a modified expression of Lee, Thring and Beer (53), namely,

$$\frac{dC_s}{dt} = C_{s0} \left[1 - 0.2713 \times 10^{10} \frac{400}{d_0} t \left(p_{O_2}^a / \sqrt{T} \right) \exp(-39,500/RT) \right] \quad (13)$$

where $a = 1$ for $T \leq 1600$ °K and $p_{O_2} \leq 0.1$ atm and $a \rightarrow 0$ as $T \rightarrow 2500$ °K and $p_{O_2} \rightarrow 1$ atm. The second choice is to use the Nagle and Strickland - Constable (60) formula.

B. FUEL OXIDATION

The oxidation of both long chain and cyclic hydrocarbons has been treated previously by Edelman, Fortune and Weilerstein (61) using a quasi-global model. This model is illustrated in Table V where both kinetic mechanism and Arrhenius rates are presented.

In the context of the present study, the oxidation reactions associated with the pyrolysis reactions (8) and (9) would be:



For those reactions, the rates can be expressed according to Ref. (61):

$$\frac{dC_{F_1}}{dt} = -A_3 T^{b_1} p^{c_1} C_{O_2}^{\alpha_1} C_{F_1}^{\beta_1} \exp(-E_3/RT) \quad (16)$$

$$\frac{dC_{F_2}}{dt} = -A_4 T^{b_2} p^{c_2} C_{O_2}^{\alpha_2} C_{F_2}^{\beta_2} \exp(-E_4/RT) \quad (17)$$

where the values of A_3 , A_4 , E_3 , E_4 , b_1 , b_2 , c_1 , c_2 , α_1 , α_2 , β_1 and β_2 would be based initially on values given in Table V, and subsequently extended for the multistep reactions (16) and (17) in conjunction with experiments to be conducted in the well-stirred reactor.

In conclusion, it is clear that the major experimental effort should be directed towards (1) measuring Arrhenius parameters for the

pyrolysis and oxidative pyrolysis of hydrocarbon mixtures, (2) determining the size distribution of soot particles, and the global rates of soot formation during pyrolysis of the above fuels, and (3) providing Arrhenius parameters for the global reaction rates of fuel oxidation in conjunction with fuel pyrolysis. It appears that sufficient information on soot oxidation rates is currently available to permit the initial development of the overall quasi-global model. Table VI summarizes all of the above information.

TABLE IV

REFERENCE	SUBSTANCE USED	INITIAL PARTICLE SIZE, A	P_{O_2} atm	T °K	K_s g/cm ² sec atm	K	A	E cal/mole
55	Solid carbon	large ($\approx 1.25 \times 10^8$)	0.0025-0.2	900-1500	A exp (-E/RT)	computed at 1600°K: 7.42×10^6	4.64×10^4	40,000
56	Solid carbon	30×10^4 - 1.25×10^8	0.02 - 0.33	900-1800	A exp (-E/RT)	computed at 1600°K: 1.39×10^6	8.71×10^3	35,700
53	Soot	400	0.02 - 0.12	1300 - 1600	K exp (-E/RT) / T ^{1/2}	1.085×10^4	computed at 1600°K 250	39,300
54	Soot	150 - 500 $R_m = 200-300$	(unclear 1.5%-6% concentration)	1200-2000	K exp (-E/RT) / T ^{1/2}	7.5×10^4	computed at 1600°K 1875	39,300
57	Soot	$R_m = 45-180$.05-13	1700-4000	$12 \left\{ \begin{aligned} &20 \exp(-15,100/T) / \\ &[(1+21.3 \exp(2,060/T) \\ &P_{O_2})(1+33.86 \exp \\ &(-41,160/T) P_{O_2}^{-1})] \\ &+4.46 \times 10^{-3} \exp(-7,060/T) \times [1-(1+33.86 \exp \\ &(-41,160/T) P_{O_2}^{-1})^{-1}] \end{aligned} \right\}$			

Table V. Extended C-H-O chemical kinetic reaction mechanism $k_f = A P^b \exp(-E/RT)$

Reaction	A		Forward b	E/R	
	Long Chain	Cyclic		Long Chain	Cyclic
1) $C_n H_m + \frac{n}{2} O_2 \rightarrow \frac{m}{2} H_2 + n CO$ ^a	6.0×10^4	2.08×10^7	1	12.2×10^3	19.65×10^3
2) $CO + OH = H + CO_2$	5.6×10^{11}		0	$.543 \times 10^3$	
3) $CO + O_2 = CO_2 + O$	3×10^{12}		0	25.0×10^3	
4) $CO + O + M = CO_2 + M$	1.8×10^{19}		-1	2×10^3	
5) $H_2 + O_2 = OH + OH$	1.7×10^{13}		0	24.7×10^3	
6) $OH + H_2 = H_2O + H$	2.19×10^{13}		0	2.59×10^3	
7) $OH + OH = O + H_2O$	5.75×10^{12}		0	$.393 \times 10^3$	
8) $O + H_2 = H + OH$	1.74×10^{13}		0	4.75×10^3	
9) $H + O_2 = O + OH$	2.24×10^{14}		0	8.45×10^3	
10) $M + O + H = OH + M$	1×10^{16}		0	0	
11) $M + O + O = O_2 + M$	9.38×10^{14}		0	0	
12) $M + H + H = H_2 + M$	5×10^{15}		0	0	
13) $M + H + OH = H_2O + M$	1×10^{17}		0	0	
14) $O + N_2 = N + NO$	1.36×10^{14}		0	3.775×10^4	
15) $N_2 + O_2 = N + NO_2$	2.7×10^{14}		-1.0	6.06×10^4	
16) $N_2 + O_2 = NO + NO$	9.1×10^{24}		-2.5	6.46×10^4	
17) $NO + NO = N + NO_2$	1.0×10^{10}		0	4.43×10^4	
18) $NO + O = O_2 + N$	1.55×10^9		1.0	1.945×10^4	
19) $M + NO = O + N + M$	2.27×10^{17}		-0.5	7.49×10^4	
20) $M + NO_2 = O + NO + M$	1.1×10^{16}		0	3.30×10^4	
21) $M + NO_2 = O_2 + N + M$	6.0×10^{14}		-1.5	5.26×10^4	
22) $NO + O_2 = NO_2 + O$	1×10^{12}		0	2.29×10^4	
23) $N + OH = NO + H$	4×10^{13}		0	0	
24) $H + NO_2 = NO + OH$	3×10^{13}		0	0	
25) $CO_2 + N = CO + NO$	2×10^{11}		-1/2	4×10^3	
26) $CO + NO_2 = CO_2 + NO$	2×10^{11}		-1/2	2.5×10^3	

$$^a \frac{dC_{C_n H_m}}{dt} = -A T^b P^{0.3} C_{C_n H_m}^{1/2} C_{O_2} \exp\left(-\frac{E}{RT}\right); [C] = \frac{\text{gm. moles}}{\text{cc}}, [T] = ^\circ K, [P] = \text{atm.}, [E] = \frac{\text{k cal}}{\text{mole}}$$

TABLE VI

QUASI-GLOBAL REACTIONS	REACTION RATES	REFERENCES	INFORMATION NEEDED	PRIORITY
<p><u>Fuel Pyrolysis and soot formation</u></p> $F_1 + M \rightarrow F_2 + M + \alpha (F_1, F_2)H_2 + NX$ $F_2 + M \rightarrow C_s + H_2 + M$	$\frac{dC_{F_1}}{dt} = -A_1 C_{F_1} \exp(-E/RT)$ $\frac{dC_{F_2}}{dt} = -A_2 C_{F_2} \exp(-E_2/RT)$	<p>1-4 and 7-15</p>	<p>A_1, A_2 E_1, E_2</p>	<p>First priority</p>
<p><u>Fuel Oxidation</u></p> $F_1 + O_2 \rightarrow CO + H_2$ $F_2 + O_2 \rightarrow CO + H_2$	$\frac{dC_{F_1}}{dt} = -A_3 T^{b_1} p^{c_1} C_{O_2}^{\alpha_1} C_{F_1}^{\beta_1} \exp(-E_3/RT)$ $\frac{dC_{F_2}}{dt} = -A_4 T^{b_1} p^{c_1} C_{O_2}^{\alpha_1} C_{F_1}^{\beta_2} \exp(-E_4/RT)$	<p>61</p>	<p>$A_3, A_4, E_3,$ $E_4, b_1, b_2,$ $c_1, c_2, \alpha_1,$ $\alpha_2, \beta_1, \beta_2$</p>	<p>Second priority</p>
<p><u>Soot Oxidation</u></p> $C_s + O_2 \rightarrow CO_2$	$\frac{dC_s}{dt} = C_s \left[1 - 0.2713 \times 10^{10} \frac{400}{d_o} t \left(\frac{p_{O_2}^a}{\sqrt{T}} \right) \exp\left(-\frac{39,300}{RT}\right) \right]$ <p>where $a = 1$ for $T \leq 1600$ °K and $p_{O_2} \leq 0.1$ atm $a \rightarrow 0$ as $T \rightarrow 2500$ °K and $p_{O_2} \rightarrow 1$ atm or the Nagle and Strickland-Constable (60) expression of Table IV</p>	<p>55-60</p>	<p>Initially none</p>	<p>- 134 -</p>

REFERENCES

1. Chinitz, W., "On the Pyrolysis of Hydrocarbon Fuels," Technical memo #153 prepared by GASL, Inc., Westbury, L.I., New York (1966)
2. Skinner, G. B. and Ruehrwein, R. A., J. Phys. Chem., 63, 1736 (1959).
3. Chen, C. J., Back, M. H. and Back R. A., "Mechanism of the Thermal Decomposition of Methane," Industrial and Laboratory Pyrolysis, Editors Albright, L. F. and Crynes, B. L., ACS Symposium series 32, p. 1, Washington, D.C. (1976)
4. Skinner, G. B. and Ball W. E., J. Phys. Chem., 64, 1025, (1960).
5. Gardiner, W. C., et.al., "Rate Mechanism of Methane Pyrolysis from 2000 to 2700 K," 15th Symposium International on Combustion, 857 (1974).
6. Back, M. H., "Pyrolysis of Hydrocarbons," NBS Special Publication 357, Editor, Wall, L. A., (1972)
7. Quinn, C. P., Proc. Roy. Soc. A257, 190 (1963).
8. Gordon, A. S., CIC Symposium on the kinetics of pyrolytic reactions, Ottawa (1964).
9. Lin, M. C. and Back M. H., Can. J. Chem., 44, 505 (1966).
10. Dunkleman, J. J. and Albright, L. F., "Surface Effects During Pyrolysis of Ethane in Tubular Flow Reactors," Industrial and Laboratory Pyrolysis, Editor Albright, L. F. and Crynes B. L., p. 241, ACS Symposium Series 32, Washington, D.C. (1976).
11. Trenwith, A. B., Trans. Faraday Soc., 62, 1538 (1966)
12. Davis, H. G. and Williamson, K. D., 5th World Petroleum Congress (1959), Section IV, p.37.
13. Laidler, K. J. and Wojciechowski, B. W., Proc. Roy. Soc. (London), A260, 91 (1961).
14. Taylor, J. E. and Kulich, D. M., "Oxidative Pyrolysis of Selected Hydrocarbons Using the Wall-less Reactor," Industrial and Laboratory Pyrolysis, Editors Albright, L. F. and Crynes B. L., ACS Symposium Series 32, p. 72, Washington, D. C. (1976).
15. Williamson, K. D. and Davis, H. G., "Mechanistic Studies of Ethane Pyrolysis at Low Pressures," Industrial and Laboratory Pyrolysis, Editors, Albright, L. F. and Crynes, B. L., ACS Symposium Series 32, p. 51, Washington, D.C. (1976).
16. Boyd, M. L., Wu, T. M. and Back, M. H., Can. J. Chem., 46, 2415 (1968).

17. Halstead, M. P. and Quinn, C. P., Trans. Faraday Soc. 64, 103 (1968).
18. Kallend, A. S., Purnell, J. H. and Shurlock, B. C., Proc. Roy. Soc., A300, 120 (1967).
19. Murgulescu, I. G. and Bică, I., "Pyrolysis and Oxidative Pyrolysis of Isobutene, I," Rev. Roum. de Chimie, 19 (12), 1841 (1974).
20. Golden, D. M., "Pyrolysis and Oxidation of Aromatic Compounds," Paper presented at Project Squid Workshop on Alternative Hydrocarbon Fuels for Engines: Combustion and Chemical Kinetics, Sept. 7-9, 1977, Loyolla College Conference Center, Columbia, Maryland.
21. Caretto, L. S., "Modeling the Gas Phase Kinetic of Fuel Nitrogen," Presented at the Western States Section, Spring Meeting, University of Utah, Salt Lake City, Utah, April, 1976.
22. Bradley, J. N. and Durden, D. A., "The Role of Pyrolysis Reactions in Hydrocarbon Oxidation," Combustion and Flame, 19, 452 (1972).
23. Leadova, Iu. I, Vedenev, V. I. and Voevodskii, V. V., Doklady Akad. Nauk. SSSR, 114, 1269 (1957).
24. Molera, M. J. and Stubbs, F. J., J. Chem Soc. 38 (1952).
25. Hausmann, E. D. and King, C. J., Ind. and Eng. Chem. (Fundamentals), 5, 295 (1966).
26. Appleby, W. D., Avery, W. H., Meerbot, W. K. and Sartor, A. F., J. Amer. Chem. Soc., 75, 1809 (1953).
27. Palmer, H. B. and Cullis, C. F., "The Formation of Carbon from Gases," Chemistry and Physics of Carbon, Vol. 1, p. 265, Editor Walker, P. L. Jr.
28. Smith, E. C. W., Proc. Roy. Soc. (London), A174, 110 (1940).
29. Gaydon, A. G., and Wolfhard, H. G., Flames, 2nd ed., Chapman and Hall, London, 1960, Chap. VIII.
30. Cabannes, F., J. Phys. Radium, 17, 492 (1956).
31. Porter, G., Symp. Comb. 4th, Cambridge, Mass., 1952, 248 (1953).
32. Porter, G., Combustion Researches and Reviews, Butterworth and Co., London, 108, 1955.
33. Anderson, R. C., Literature of the Combustion of Petroleum, American Chemical Soc., Washington, 49 (1958).
34. Street, J. C. and Thomas, A., Fuel, 34, 4 (1955).
35. Tesner, P. A., Symp. Comb. 7th, London, Oxford, 1958, 546 (1959)
36. Behrens, H., Z. Physik. Chem., 199, 1, (1952).

37. Behrens, H., Symp. Combust., 4th, Cambridge, Mass, 1952, 538 (1953)
38. Homann, K. H., "Carbon Formation in Premixed Gases," NBS Special Publication 357, 143 (1972).
39. Homann, K. H., "Carbon Formation in Premixed Flames," Combustion and Flames, II, 265 (1967).
40. Wright, F. J., "The Formation of Carbon Under Well-Stirred Conditions," 12th International Symposium on Combustion, 867 (1969).
41. Scully, D. B. and Davies, R. A., "Carbon Formation from Aromatic Hydrocarbons," Combustion and Flame, 9, 185 (1965).
42. Davies, R. A. and Scully, D. B., "Carbon Formation from Aromatic Hydrocarbons II," Combustion and Flame, 10, 165 (1966).
43. Homann, K. H. and Wagner, H. Gg., "Some Aspects of the Mechanism of Carbon Formation in Premixed Flames," 11th International Symposium on Combustion, 371, (1967).
44. D'Alesio, A., Di Lorenzo, A., Sarofim, A. F., Beretta, F., Masi, S. and Venitozzi, C., "Soot Formation in Methane-Oxygen Flames," 15th International Symposium on Combustion, 1427 (1974).
45. Macfarlane, J. J., Holderness, F. H. and Witcher, F. S. E., "Soot Formation Rates in Premixed C₅ and C₆ Hydrocarbon-Air Flames at Pressures up to 20 Atmospheres," Combustion and Flame, 8, 215 (1964).
46. Howard, J. B., "On the Mechanism of Carbon Formation in Flames," 12th Symposium International on Combustion, The Combustion Institute, 877 (1969).
47. Ball, R. T. and Howard, J. B., "Electric Charge of Carbon Particles in Flames," 13th Symposium International on Combustion, The Combustion Institute, 353 (1971).
48. Wersborg, B. L., Howard, J. B. and Williams, G. C., "Physical Mechanisms in Carbon Formation in Flames," 14th Symposium (International) on Combustion, The Combustion Institute, 923 (1973).
49. Howard, J. B., Wersborg, B. L. and Williams, G. C., "Coagulation of Carbon Particles in Premixed Flames," Faraday Symposia of the Chemical Society, 7, 109 (1973)
50. Wersborg, B. L., Yeung, A. C. and Howard, J. B., "Concentration and Mass Distribution of Charged Species in Sooting Flames," 15th Symposium International on Combustion, The Combustion Institute, 1437 (1974).
51. Homann, K. H., Discussion of paper of Place E.R. and Weinberg F. J., "The Nucleation of Flame Carbon by Ions and the Effect of Electric Fields," 11th Symposium International on Combustion, 254 (1967), The Combustion Institute.

52. Jensen, D. E., "Prediction of Soot Formation Rates: A New Approach," Proc. Roy. Soc. (London) A338, 375 (1974).
53. Lee, K. B., Thring, M. W. and Beer, J. M., "On the Rate of Combustion of Soot in a Laminar Soot Flame," Combustion and Flame, 6, 137 (1962)
54. Kahn, I. M., Wang, C, H. T. and Langridge, B. E., "Coagulation and Combustion of Soot Particles in Diesel Engines," Combustion and Flame, 17, 409 (1971)
55. Parker, A. S. and Hottel, H. C., Ind. Eng. Chem., 28,1334 (1936).
56. Field, M. A., Gill, D. W., Morgan, B. B. and Hawksley, P. G. W., Combustion of Pulverized Coal, British Coal Utilization Research Association: Leatherhead, England (1967).
57. Park, C and Appleton, J. P., "Shock-Tube Measurements of Soot Oxidation Rates," Combustion and Flame, 20, 369 (1973).
58. Fenimore, C. P. and Jones, G. W., J. Phys. Chem., 71, 593 (1971)
59. Tenser, P. A. and Tsibulevsky, A. M., Combustion, Explosions and Shock-Waves, 3, 163 (1967).
60. Nagle, J. and Strickland - Constable, R. F., Proc. Fifth Carbon Conf., 1, 154 (1962).
61. Edelman, R. B., Fortune, O., and Weilerstein, G., "Some Observations on Flows Described by Coupled Mixing and Kinetics," Emissions From Continuous Combustion Systems, p. 55. Editors Walter Cornelius and William G. Agnew, Plenum Press (1972).

SATISFACTION GUARANTEED

NTIS strives to provide quality products, reliable service, and fast delivery. Please contact us for a replacement within 30 days if the item you receive is defective or if we have made an error in filling your order.

▶ **E-mail: info@ntis.gov**

▶ **Phone: 1-888-584-8332 or (703)605-6050**

Reproduced by NTIS

National Technical Information Service
Springfield, VA 22161

This report was printed specifically for your order from nearly 3 million titles available in our collection.

For economy and efficiency, NTIS does not maintain stock of its vast collection of technical reports. Rather, most documents are custom reproduced for each order. Documents that are not in electronic format are reproduced from master archival copies and are the best possible reproductions available.

Occasionally, older master materials may reproduce portions of documents that are not fully legible. If you have questions concerning this document or any order you have placed with NTIS, please call our Customer Service Department at (703) 605-6050.

About NTIS

NTIS collects scientific, technical, engineering, and related business information – then organizes, maintains, and disseminates that information in a variety of formats – including electronic download, online access, CD-ROM, magnetic tape, diskette, multimedia, microfiche and paper.

The NTIS collection of nearly 3 million titles includes reports describing research conducted or sponsored by federal agencies and their contractors; statistical and business information; U.S. military publications; multimedia training products; computer software and electronic databases developed by federal agencies; and technical reports prepared by research organizations worldwide.

For more information about NTIS, visit our Web site at <http://www.ntis.gov>.

NTIS

**Ensuring Permanent, Easy Access to
U.S. Government Information Assets**



U.S. DEPARTMENT OF COMMERCE
Technology Administration
National Technical Information Service
Springfield, VA 22161 (703) 605-6000
